Journal of Computational and Applied Mathematics 291 (2016) 158–182

Contents lists available at ScienceDirect

Journal of Computational and Applied Mathematics

journal homepage: www.elsevier.com/locate/cam

Unconditionally stable methods for simulating multi-component two-phase interface models with Peng–Robinson equation of state and various boundary conditions☆

Jisheng Kou [a], Shuyu Sun [b,c,*]

[a] School of Mathematics and Statistics, Hubei Engineering University, Xiaogan 432000, Hubei, China

[b] Computational Transport Phenomena Laboratory, Division of Physical Science and Engineering, King Abdullah University of Science and Technology, Thuwal 23955-6900, Saudi Arabia

[c] School of Mathematics and Statistics, Xi'an Jiaotong University, Xi'an 710049, China

ARTICLE INFO

Article history:
Received 31 August 2014
Received in revised form 11 February 2015

MSC:
65N30
65N50
49S05

Keywords:
Two-phase interfaces
Multi-component fluids
Peng–Robinson equation of state
Cahn–Hilliard system
Unconditional stability

ABSTRACT

In this paper, we consider multi-component dynamic two-phase interface models, which are formulated by the Cahn–Hilliard system with Peng–Robinson equation of state and various boundary conditions. These models can be derived from the minimum problems of Helmholtz free energy or grand potential in the realistic thermodynamic systems. The resulted Cahn–Hilliard systems with various boundary conditions are fully coupled and strongly nonlinear. A linear transformation is introduced to decouple the relations between different components, and as a result, the models are simplified. From this, we further propose a semi-implicit unconditionally stable time discretization scheme, which allows us to solve the Cahn–Hilliard system by a decoupled way, and thus, our method can significantly reduce the computational cost and memory requirements. The mixed finite element methods are employed for the spatial discretization, and the approximate errors are also analyzed for both space and time. Numerical examples are tested to demonstrate the efficiency of our proposed methods.

1. Introduction

The subsurface oil and gas reservoirs typically contain oil phase, gas phase and water phase, together with the solid phase (rock or soil) [1], so it has been a major issue to simulate multiphase fluid systems in reservoir engineering [2–7]. For understanding physical phenomena, such as liquid droplets, gas bubbles, phase interfaces, and capillary pressure, it is necessary to model and simulate the interface between phases.

As a popular methodology modeling the multi-phase interface, diffuse interface models have been extensively studied in the literature, for example, [8–16]. In these works, a simple double-well potential is usually employed (thus simulation

☆ This work is supported by National Natural Science Foundation of China (No. 11301163), the Key Project of Chinese Ministry of Education (No.212109) and the KAUST research fund.

* Corresponding author at: Computational Transport Phenomena Laboratory, Division of Physical Science and Engineering, King Abdullah University of Science and Technology, Thuwal 23955-6900, Saudi Arabia.

E-mail address: shuyu.sun@kaust.edu.sa (S. Sun).

http://dx.doi.org/10.1016/j.cam.2015.02.037
0377-0427/

being only qualitative) rather than a more realistic equation of state (e.g. Peng–Robinson equation of state [17]), and the latter is more accurate but computationally more challenging. However, it is not possible to use quantitatively meaningful parameters of a simple double-well potential for simulation of realistic hydrocarbon species in an oil–gas two-phase system [18,19].

In our previous work [18,20], we have studied the static solution of the diffuse interface model with Peng–Robinson equation of state for multi-component fluid system to calculate the surface tension. Moreover, the kinetics of phase transformation is also important for controlling the microstructures of multi-component systems in many practical applications [21–26]. The Cahn–Hilliard equation [21] is a better approach to simulate the dynamics of the two-phase fluid system since it carries more physics (correct diffusion) than the static model.

Consider a mixture composed of $N(N \geq 2)$ components and denote the mixture composition by $\mathbf{n} = [n_1, n_2, \ldots, n_N]^T$, where n_i is the molar density of the ith component. In non-ideal multi-component chemical systems, the driving force for diffusion of each component is the gradient of chemical potential of this component, and thus, Fick's first law for each component gives us

$$\boldsymbol{J}_i = -\mathcal{M}(\mathbf{n})\nabla\mu_i, \quad i = 1, \ldots, N, \tag{1.1}$$

where $\boldsymbol{J}_i$ is the flux of component i, $\mathcal{M}(\mathbf{n}) > 0$ is the diffusivity, and μ_i is the chemical potential of component i. Although the diffusivity $\mathcal{M}$ may be a tensor and $\boldsymbol{J}_i$ may also depend on the chemical potential gradients of other components, we only focus on the case where diffusivity is a scalar quantity and assume that all components have the same diffusivity.

Suppose that the influence parameter c_{ij} is independent of molar density, and then the chemical potential of the ith component in an inhomogeneous fluid is calculated as [19]

$$\mu_i = \mu_i^0(\mathbf{n}) - \sum_{j=1}^{N} c_{ij}\Delta n_j, \quad i = 1, \ldots, N, \tag{1.2}$$

where μ_i^0 is the chemical potential of the ith component in a homogeneous fluid defined as

$$\mu_i^0 = \left(\frac{\partial f_0(\mathbf{n})}{\partial n_i}\right)_{T, n_1, \ldots, n_{i-1}, n_{i+1}, \ldots, n_N}. \tag{1.3}$$

In (1.3), T represents the temperature, and $f_0(\mathbf{n})$ is the Helmholtz free energy density of a homogeneous fluid (its definition can be found in the Appendix of this paper). The pure component influence parameters c_i is calculated by the formulae given in the Appendix of this paper. The crossed influence parameters c_{ij} in (1.2) is generally described as the modified geometric mean of the pure component influence parameters c_i and c_j by

$$c_{ij} = (1 - \beta_{ij})\sqrt{c_i c_j}, \tag{1.4}$$

where the parameters β_{ij} are binary interaction coefficients for the influence parameters. The dependence of the influence parameters on the component density is neglected [27], and thus their values are independent of spatial positions. The influence parameter matrix is denoted by $\mathbf{C} = \left(c_{ij}\right)_{i,j=1}^{N}$. In this paper, the suitable parameters β_{ij} are chosen such that $\mathbf{C}$ is symmetrical positive definite.

The mass conservation law is applied for component i to arrive at

$$\frac{\partial n_i}{\partial t} + \nabla \cdot \boldsymbol{J}_i = 0, \quad i = 1, \ldots, N. \tag{1.5}$$

Thus, the system of Cahn–Hilliard equations for multi-component models with the Peng–Robinson equation of state is described as a combination of (1.1), (1.2) and (1.5).

In the realistic thermodynamic system, the minimum problems of both Helmholtz free energy and grand potential can result in the above Cahn–Hilliard system with different boundary conditions [1,24,28]. We will discuss four types of boundary conditions for the Cahn–Hilliard equations and establish the relation between these problems and the corresponding minimum formulations. To our knowledge, it has not been conducted to simulate multi-component dynamic two-phase interface problems by using the Cahn–Hilliard equations with Peng–Robinson equation of state and various boundary conditions.

The multi-component interface models considered in this paper are fully coupled and strongly nonlinear systems of Cahn–Hilliard equations, which has N unknown density variables. It is a key issue for efficiently simulating this system to design the stable time discretization methods with less computations. There are many numerical studies with phase-field models [29,14,30,31,26,16,32,15,33–38]. To avoid a severe time step restriction for numerical stability, the fourth-order spatial derivatives are often treated by the implicit time scheme. However, this treatment will cause huge computational costs and memory requirement since we need to solve N density variables simultaneously. To overcome this computational challenge, we will introduce a linear transformation to decouple the relations between different component densities, and thus, our method significantly reduces the computational cost and memory requirements.

The other computational challenge results from the strong nonlinearity of μ_i^0 and the fact that the influence parameters c_{ij} is relatively small. The numerical experiments show that the fully explicit time scheme for μ_i^0 works not well since it

demands very small time steps to guarantee the stability. The fully implicit time scheme for μ_i^0 is not a good choice; in fact, for this case, we yet need to solve N density variables simultaneously because of the full coupling and strong nonlinearity of μ_i^0 as the functions of component densities. In this paper, we pay our attention to the semi-implicit time marching schemes, which have been shown to be attractive in the literature. For the N-component Cahn–Hilliard system modeling the phase separation of an N-component mixture, but which is not modeled by Peng–Robinson equation of state, a unconditionally stable numerical scheme has been proposed in [26] and the N-component Cahn–Hilliard system is solved in a decoupled way. But this approach cannot decouple the relations between the component densities of our model because of the complication of Peng–Robinson equation of state. In this paper, we will propose a semi-implicit unconditionally stable time scheme based on the introduced linear transformation, and moreover, this scheme is also consistent with the decoupling approach used for spatial derivatives.

For the spatial discretization, we use the mixed finite element (MFE) methods [39–41], which have been used frequently in reservoir engineering problems for the reasons that they are capable to achieve very accurate and stable approximations of both the primary unknown and its flux across grid-cell interfaces. The MFE methods have also the local mass conservation property, which is preferable for component mass conservative problems. We must note that the mixed formulations are very different from those used frequently in the literature, for example, [36,26,16]. In fact, our mixed formulations are similar to those used in the local discontinuous Galerkin methods [34,35], but our formulations employ the mixed finite element spaces instead of discontinuous basis functions.

The rest of this paper is organized as follows. In Section 2, we will introduce the diffuse interface models with different boundary conditions, and we also introduce a linear transformation to simplify these model formulations. In Section 3, the mixed forms of the Cahn–Hilliard system will be introduced and the corresponding energy/potential decreasing property is proved. In Section 4, the semi-implicit time marching schemes will be developed and the unconditional stability will be proved. In Section 5, we will describe mixed finite element approximations of our models and analyze approximate errors of both space and time. In Section 6, numerical examples are given to verify the theoretical results and the efficiency of the proposed methods. Finally, concluding remarks are provided in Section 7.

2. Mathematical models

2.1. Model problems with different boundary conditions

Suppose that $\Omega \subset \mathbf{R}^d (1 \leq d \leq 3)$ is an open, bounded and connected domain containing the two-phase fluid interface, and the boundary $\partial\Omega$ is sufficiently smooth. Moreover, both gas and liquid regions within Ω are not empty. Let $\boldsymbol{\nu}_{\partial\Omega}$ be the outward normal to the boundary $\partial\Omega$. The Neumann–Neumann type boundary conditions are given by

$$\nabla n_i \cdot \boldsymbol{\nu}_{\partial\Omega} = 0, \qquad \boldsymbol{J}_i \cdot \boldsymbol{\nu}_{\partial\Omega} = 0, \quad i = 1, \ldots, N. \tag{2.1}$$

The Dirichlet–Neumann type boundary conditions are given by

$$n_i = n_i^B, \qquad \boldsymbol{J}_i \cdot \boldsymbol{\nu}_{\partial\Omega} = 0, \quad i = 1, \ldots, N. \tag{2.2}$$

The Neumann–Dirichlet type boundary conditions are given by

$$\nabla n_i \cdot \boldsymbol{\nu}_{\partial\Omega} = 0, \qquad \mu_i = \mu_i^B, \quad i = 1, \ldots, N. \tag{2.3}$$

The Dirichlet–Dirichlet type boundary conditions are given by

$$n_i = n_i^B, \qquad \mu_i = \mu_i^B, \quad i = 1, \ldots, N. \tag{2.4}$$

Here, we assume that μ_i^B is a constant on the whole boundary $\partial\Omega$. Moreover, all boundary conditions are assumed to be independent of time.

In order to simplify the norm notation in this paper, we use $\|\cdot\|$ to indicate the norms in the function space $L^2(\Omega)$ or vector function space $\left(L^2(\Omega)\right)^d$. In the absence of an external potential, we define the Helmholtz free energy of an inhomogeneous fluid as

$$H = \int_\Omega \left(f_0(\mathbf{n}) + \frac{1}{2} \sum_{i,j=1}^{N} c_{ij} \nabla n_i \cdot \nabla n_j \right) d\mathbf{x}, \tag{2.5}$$

which is the sum of two contributions: the Helmholtz energy $f_0(\mathbf{n})$ of homogeneous fluid at local composition $\mathbf{n}$, and a corrective term that is a function of the local density gradients. For the problems with the Neumann–Neumann and Dirichlet–Neumann boundary conditions, the total mass of each component is conserved since

$$\frac{\partial}{\partial t} \int_\Omega n_i d\mathbf{x} = 0, \quad i = 1, \ldots, N. \tag{2.6}$$

We first multiply (1.5) by μ_i, taking into account (1.1) and (1.2), then integrate it over Ω and sum it by i to reach

$$\frac{\partial H}{\partial t} = -\sum_{i=1}^{N} \left\| \mathcal{M}(\mathbf{n})^{1/2} \nabla \mu_i \right\|^2. \tag{2.7}$$

The total mass of each component may be not conserved for the problems with the Neumann–Dirichlet and Dirichlet–Dirichlet boundary conditions; in fact, because of the gradients of chemical potential, the mass transfer of each component often occurs between these fluid systems and outside fluids unless they attain the equilibrium. For these two cases of boundary conditions, we define the grand potential of an inhomogeneous fluid as

$$G = \int_\Omega \left(f_0(\mathbf{n}) - \sum_{i=1}^N \mu_i^B n_i + \frac{1}{2} \sum_{i,j=1}^N c_{ij} \nabla n_i \cdot \nabla n_j \right) d\mathbf{x}. \tag{2.8}$$

We first multiply (1.5) by $\left(\mu_i - \mu_i^B\right)$, and similar to (2.7), we have

$$\frac{\partial G}{\partial t} = -\sum_{i=1}^N \left\| \mathcal{M}(\mathbf{n})^{1/2} \nabla \mu_i \right\|^2. \tag{2.9}$$

It is noted that unlike the Helmholtz free energy, the grand potential of a mixture may be negative, but it is always decreasing until this mixture reaches to the equilibrium states with given chemical potentials.

2.2. Transformed variables

The influence matrix $\mathbf{C}$ is symmetrical positive definite, so there exist N real positive eigenvalues λ_i of $\mathbf{C}$, and the corresponding normal orthonormal eigenvectors, denoted by $\mathbf{v}_i$, $1 \le i \le N$. Define a transformation matrix $\mathbb{Q} = [\mathbf{v}_1, \ldots, \mathbf{v}_N]$, which is orthogonal. Using this orthonormal transformation, we define a vector $\mathbf{u} = [u_1, u_2, \ldots, u_N]^T$ as

$$\mathbf{u} = \mathbb{Q}^T \mathbf{n}, \quad \mathbf{n} = \mathbb{Q}\mathbf{u}. \tag{2.10}$$

For the regularity relation between $\mathbf{u}$ and $\mathbf{n}$, we have the following lemma.

Lemma 2.1. *If* $\mathbf{u} \in (H^s(\Omega))^N$ $(s \ge 0)$, *then* $\mathbf{n} \in (H^s(\Omega))^N$, *and vice versa.*

Proof. The proof can be obtained immediately from the property of the linear transformation. □

2.3. Transformed models

Denote $g_0(\mathbf{u}) = f_0(\mathbf{n}) = f_0(\mathbb{Q}\mathbf{u})$. Using the relations given by (2.10), we get

$$\sum_{i,j=1}^N c_{ij} \nabla n_i \cdot \nabla n_j = \sum_{i=1}^N \lambda_i |\nabla u_i|^2. \tag{2.11}$$

The Helmholtz free energy (2.5) can be rewritten as

$$H = \int_\Omega \left(g_0(\mathbf{u}) + \frac{1}{2} \sum_{i=1}^N \lambda_i |\nabla u_i|^2 \right) d\mathbf{x}. \tag{2.12}$$

Let $\boldsymbol{\mu}_B = [\mu_1^B, \ldots, \mu_N^B]^T$. The grand potential of an inhomogeneous fluid can also be rewritten as

$$G = \int_\Omega \left(g_0(\mathbf{u}) - \boldsymbol{\mu}_B^T \mathbb{Q}\mathbf{u} + \frac{1}{2} \sum_{i=1}^N \lambda_i |\nabla u_i|^2 \right) d\mathbf{x}. \tag{2.13}$$

With the above transformation, the Cahn–Hilliard system considered in this paper, along with the boundary conditions, can also be reformulated similarly, but we drop their expressions for sake of brevity.

3. Mixed forms of the Cahn–Hilliard system

The Raviart–Thomas mixed finite element methods have been extensively used for solving the elliptic and parabolic equations. In order to use these methods, based on the transformed variables stated in Section 2, we need to reform the Cahn–Hilliard system considered in this paper, along with the boundary conditions, into a mixed form. Let $\boldsymbol{\mu}^0 = [\mu_1^0, \ldots, \mu_N^0]^T$. The mixed form of the transformed Cahn–Hilliard equation with the Neumann–Neumann and Dirichlet–Neumann type boundary conditions is expressed as

$$\frac{\partial u_i}{\partial t} + \nabla \cdot \boldsymbol{w}_i = 0, \tag{3.1a}$$

$$\mathcal{M}(\mathbf{n})^{-1} \boldsymbol{w}_i = -\nabla q_i, \tag{3.1b}$$

$$\lambda_i \nabla \cdot \boldsymbol{s}_i + \mathbf{v}_i^T \boldsymbol{\mu}^0(\mathbf{n}) = q_i, \tag{3.1c}$$

$$\boldsymbol{s}_i = -\nabla u_i, \tag{3.1d}$$

where $i = 1, \ldots, N$. Denote $u_i^B = \mathbf{v}_i^T \mathbf{n}^B$. For the system given by (3.1), the Neumann–Neumann type boundary conditions become $\boldsymbol{s}_i \cdot \boldsymbol{\nu}_{\partial\Omega} = 0$ and $\boldsymbol{w}_i \cdot \boldsymbol{\nu}_{\partial\Omega} = 0$, while the Dirichlet–Neumann type boundary conditions become $u_i = u_i^B$ and $\boldsymbol{w}_i \cdot \boldsymbol{\nu}_{\partial\Omega} = 0$. Based on the definition of auxiliary variables, the expression of the Helmholtz free energy becomes

$$F = \int_\Omega \left(g_0(\mathbf{u}) + \frac{1}{2} \sum_{i=1}^{N} \lambda_i |\boldsymbol{s}_i|^2 \right) d\mathbf{x}. \tag{3.2}$$

For the transformed Cahn–Hilliard equation with the Dirichlet–Dirichlet and Neumann–Dirichlet type boundary conditions, the corresponding mixed form is expressed as

$$\frac{\partial u_i}{\partial t} + \nabla \cdot \boldsymbol{w}_i = 0, \tag{3.3a}$$

$$\mathcal{M}(\mathbf{n})^{-1} \boldsymbol{w}_i = -\nabla q_i, \tag{3.3b}$$

$$\lambda_i \nabla \cdot \boldsymbol{s}_i + \mathbf{v}_i^T \boldsymbol{\mu}^0(\mathbf{n}) - q_i^B = q_i, \tag{3.3c}$$

$$\boldsymbol{s}_i = -\nabla u_i, \tag{3.3d}$$

where $i = 1, \ldots, N$ and $q_i^B = \mathbf{v}_i^T \boldsymbol{\mu}_B$. In the system given by (3.3), we always have $q_i = 0$ on the boundary Ω, but $\boldsymbol{s}_i \cdot \boldsymbol{\nu}_{\partial\Omega} = 0$ and $u_i = u_i^B$ for the Dirichlet–Dirichlet and Neumann–Dirichlet type boundary conditions, respectively. From the definition of auxiliary variables, we rewrite the expression of the grand potential as

$$G = \int_\Omega \left(g_0(\mathbf{u}) - \sum_{i=1}^{N} q_i^B u_i + \frac{1}{2} \sum_{i=1}^{N} \lambda_i |\boldsymbol{s}_i|^2 \right) d\mathbf{x}. \tag{3.4}$$

Define $H_0(\Omega; \mathrm{div}) = \{\mathbf{v} \in H(\Omega; \mathrm{div}) : \mathbf{v} \cdot \boldsymbol{\nu}_{\partial\Omega} = 0\}$. The mixed weak form of the transformed Cahn–Hilliard system with the Neumann–Neumann type boundary conditions is given as for $i = 1, \ldots, N$,

$$\left(\frac{\partial u_i}{\partial t}, \psi \right) + (\nabla \cdot \boldsymbol{w}_i, \psi) = 0, \tag{3.5a}$$

$$\left(\mathcal{M}(\mathbf{n})^{-1} \boldsymbol{w}_i, \boldsymbol{\omega} \right) = (q_i, \nabla \cdot \boldsymbol{\omega}), \tag{3.5b}$$

$$\lambda_i \left(\nabla \cdot \boldsymbol{s}_i, \varphi \right) + \left(\mathbf{v}_i^T \boldsymbol{\mu}^0(\mathbf{n}), \varphi \right) = \left(q_i, \varphi \right), \tag{3.5c}$$

$$(\boldsymbol{s}_i, \boldsymbol{\phi}) = (u_i, \nabla \cdot \boldsymbol{\phi}), \tag{3.5d}$$

where $\psi, \varphi \in L^2(\Omega)$ and $\boldsymbol{\omega}, \boldsymbol{\phi} \in H_0(\Omega; \mathrm{div})$.

Theorem 3.1. *For the case of Neumann–Neumann type boundary conditions, the Helmholtz free energy is decreased with time and satisfies*

$$\frac{\partial F}{\partial t} = -\sum_{i=1}^{N} \| \mathcal{M}(\mathbf{n})^{-1/2} \boldsymbol{w}_i \|^2. \tag{3.6}$$

Proof. By choosing $\psi = q_i$ in (3.5a) and $\boldsymbol{\omega} = \boldsymbol{w}_i$ in (3.5b), respectively, we obtain

$$\left(\frac{\partial u_i}{\partial t}, q_i \right) + (\nabla \cdot \boldsymbol{w}_i, q_i) = 0, \tag{3.7}$$

$$\| \mathcal{M}(\mathbf{n})^{-1/2} \boldsymbol{w}_i \|^2 = (q_i, \nabla \cdot \boldsymbol{w}_i), \tag{3.8}$$

where $i = 1, \ldots, N$. It is obtained by substituting (3.8) into (3.7) that

$$\left(\frac{\partial u_i}{\partial t}, q_i \right) + \| \mathcal{M}(\mathbf{n})^{-1/2} \boldsymbol{w}_i \|^2 = 0, \quad i = 1, \ldots, N. \tag{3.9}$$

For $1 \le i \le N$, the choice of $\varphi = \frac{\partial u_i}{\partial t}$ in (3.5c) gives us

$$\lambda_i \left(\nabla \cdot \boldsymbol{s}_i, \frac{\partial u_i}{\partial t} \right) + \left(\mathbf{v}_i^T \boldsymbol{\mu}^0(\mathbf{n}), \frac{\partial u_i}{\partial t} \right) = \left(q_i, \frac{\partial u_i}{\partial t} \right). \tag{3.10}$$

We first take $\boldsymbol{\phi} = \boldsymbol{s}_i$ in (3.5d)

$$\| \boldsymbol{s}_i \|^2 = (u_i, \nabla \cdot \boldsymbol{s}_i), \tag{3.11}$$

and then differentiate the above equation by the time

$$\frac{\partial}{\partial t}\|\boldsymbol{s}_i\|^2 = \left(\frac{\partial u_i}{\partial t}, \nabla\cdot\boldsymbol{s}_i\right) + \left(u_i, \nabla\cdot\frac{\partial \boldsymbol{s}_i}{\partial t}\right). \tag{3.12}$$

On the other hand, take $\boldsymbol{\phi} = \frac{\partial \boldsymbol{s}_i}{\partial t}$ in (3.5d)

$$\frac{1}{2}\frac{\partial}{\partial t}\|\boldsymbol{s}_i\|^2 = \left(u_i, \nabla\cdot\frac{\partial \boldsymbol{s}_i}{\partial t}\right). \tag{3.13}$$

It follows from (3.12) and (3.13) that

$$\frac{1}{2}\frac{\partial}{\partial t}\|\boldsymbol{s}_i\|^2 = \left(\frac{\partial u_i}{\partial t}, \nabla\cdot\boldsymbol{s}_i\right). \tag{3.14}$$

Combining (3.9), (3.10) and (3.14), we find

$$\frac{1}{2}\lambda_i\frac{\partial}{\partial t}\|\boldsymbol{s}_i\|^2 + \left(\mathbf{v}_i^T\boldsymbol{\mu}^0(\mathbf{n}), \frac{\partial u_i}{\partial t}\right) = -\|\mathcal{M}(\mathbf{n})^{-1/2}\boldsymbol{w}_i\|^2. \tag{3.15}$$

It is derived by the relation between $\mathbf{u}$ and $\mathbf{n}$ that

$$\left(\frac{\partial f_0(\mathbf{n})}{\partial t}, 1\right) = \left(\frac{\partial g_0(\mathbf{u})}{\partial t}, 1\right) = \sum_{i=1}^{N}\left(\mathbf{v}_i^T\boldsymbol{\mu}^0(\mathbf{n}), \frac{\partial u_i}{\partial t}\right). \tag{3.16}$$

Eq. (3.6) is obtained by summing (3.15) from $i = 1$ to N and taking into account (3.16). As a direct result of (3.6), the Helmholtz free energy is decreased with time. □

The mixed weak form of the transformed Cahn–Hilliard equation with the Dirichlet–Neumann type boundary conditions is expressed as for $i = 1, \ldots, N$,

$$\left(\frac{\partial u_i}{\partial t}, \psi\right) + (\nabla\cdot\boldsymbol{w}_i, \psi) = 0, \tag{3.17a}$$

$$\left(\mathcal{M}(\mathbf{n})^{-1}\boldsymbol{w}_i, \boldsymbol{\omega}\right) = (q_i, \nabla\cdot\boldsymbol{\omega}), \tag{3.17b}$$

$$\lambda_i\left(\nabla\cdot\boldsymbol{s}_i, \varphi\right) + \left(\mathbf{v}_i^T\boldsymbol{\mu}^0(\mathbf{n}), \varphi\right) = (q_i, \varphi), \tag{3.17c}$$

$$(\boldsymbol{s}_i, \boldsymbol{\phi}) = (u_i, \nabla\cdot\boldsymbol{\phi}) - \left(u_i^B, \boldsymbol{\phi}\cdot\boldsymbol{\nu}_{\partial\Omega}\right)_{\partial\Omega}, \tag{3.17d}$$

where $\psi, \varphi \in L^2(\Omega)$, $\boldsymbol{\omega} \in H_0(\Omega; \mathrm{div})$ and $\boldsymbol{\phi} \in H(\Omega; \mathrm{div})$.

Theorem 3.2. *For the case of Dirichlet–Neumann type boundary conditions, the Helmholtz free energy is decreased with time and satisfies*

$$\frac{\partial F}{\partial t} = -\sum_{i=1}^{N}\|\mathcal{M}(\mathbf{n})^{-1/2}\boldsymbol{w}_i\|^2. \tag{3.18}$$

Proof. It is similar to the proof of Theorem 3.1 that we have (3.7)–(3.10). We now take $\boldsymbol{\phi} = \boldsymbol{s}_i$ in (3.17d)

$$\|\boldsymbol{s}_i\|^2 = (u_i, \nabla\cdot\boldsymbol{s}_i) - \left(u_i^B, \boldsymbol{s}_i\cdot\boldsymbol{\nu}_{\partial\Omega}\right)_{\partial\Omega}, \tag{3.19}$$

and then differentiate the above equation by time and taking into account the independence of u_i^B on the time

$$\frac{\partial}{\partial t}\|\boldsymbol{s}_i\|^2 = \left(\frac{\partial u_i}{\partial t}, \nabla\cdot\boldsymbol{s}_i\right) + \left(u_i, \nabla\cdot\frac{\partial \boldsymbol{s}_i}{\partial t}\right) - \left(u_i^B, \frac{\partial \boldsymbol{s}_i}{\partial t}\cdot\boldsymbol{\nu}_{\partial\Omega}\right)_{\partial\Omega}. \tag{3.20}$$

It is also obtained by choosing $\boldsymbol{\phi} = \frac{\partial \boldsymbol{s}_i}{\partial t}$ in (3.17d) that

$$\frac{1}{2}\frac{\partial}{\partial t}\|\boldsymbol{s}_i\|^2 = \left(u_i, \nabla\cdot\frac{\partial \boldsymbol{s}_i}{\partial t}\right) - \left(u_i^B, \frac{\partial \boldsymbol{s}_i}{\partial t}\cdot\boldsymbol{\nu}_{\partial\Omega}\right)_{\partial\Omega}. \tag{3.21}$$

The combination of (3.20) and (3.21) leads to

$$\frac{1}{2}\frac{\partial}{\partial t}\|\boldsymbol{s}_i\|^2 = \left(\frac{\partial u_i}{\partial t}, \nabla\cdot\boldsymbol{s}_i\right). \tag{3.22}$$

The required result is obtained by the similar approaches used in the proof of Theorem 3.1. □

The mixed weak form of the transformed Cahn–Hilliard equation with the Dirichlet–Dirichlet type boundary conditions is formulated as for $i = 1, \ldots, N$,

$$\left(\frac{\partial u_i}{\partial t}, \psi\right) + (\nabla \cdot \boldsymbol{w}_i, \psi) = 0, \tag{3.23a}$$

$$\left(\mathcal{M}(\mathbf{n})^{-1}\boldsymbol{w}_i, \boldsymbol{\omega}\right) = (q_i, \nabla \cdot \boldsymbol{\omega}), \tag{3.23b}$$

$$\lambda_i (\nabla \cdot \boldsymbol{s}_i, \varphi) + \left(\mathbf{v}_i^T \boldsymbol{\mu}^0(\mathbf{n}), \varphi\right) = \left(q_i + q_i^B, \varphi\right), \tag{3.23c}$$

$$(\boldsymbol{s}_i, \boldsymbol{\phi}) = (u_i, \nabla \cdot \boldsymbol{\phi}) - \left(u_i^B, \boldsymbol{\phi} \cdot \boldsymbol{v}_{\partial\Omega}\right)_{\partial\Omega}, \tag{3.23d}$$

where $\psi, \varphi \in L^2(\Omega)$ and $\boldsymbol{\omega}, \boldsymbol{\phi} \in H(\Omega; \mathrm{div})$.

Theorem 3.3. *For the case of Dirichlet–Dirichlet type boundary conditions, the grand potential is decreased with time and satisfies*

$$\frac{\partial G}{\partial t} = -\sum_{i=1}^{N} \|\mathcal{M}(\mathbf{n})^{-1/2}\boldsymbol{w}_i\|^2. \tag{3.24}$$

Proof. It is similar to the proof of Theorem 3.1 that we have (3.9). Take $\varphi = \frac{\partial u_i}{\partial t}$ in (3.23c) for $1 \le i \le N$, we get

$$\lambda_i \left(\nabla \cdot \boldsymbol{s}_i, \frac{\partial u_i}{\partial t}\right) + \left(\mathbf{v}_i^T \boldsymbol{\mu}^0(\mathbf{n}) - q_i^B, \frac{\partial u_i}{\partial t}\right) = \left(q_i, \frac{\partial u_i}{\partial t}\right). \tag{3.25}$$

Thus, we obtain

$$\frac{1}{2}\lambda_i \frac{\partial}{\partial t}\|\boldsymbol{s}_i\|^2 + \left(\mathbf{v}_i^T \boldsymbol{\mu}^0(\mathbf{n}) - q_i^B, \frac{\partial u_i}{\partial t}\right) = -\|\mathcal{M}(\mathbf{n})^{-1/2}\boldsymbol{w}_i\|^2. \tag{3.26}$$

Since

$$\left(\frac{\partial\left(g_0(\mathbf{u}) - \sum_{i=1}^{N} q_i^B u_i\right)}{\partial t}, 1\right) = \sum_{i=1}^{N}\left(\mathbf{v}_i^T \boldsymbol{\mu}^0(\mathbf{n}) - q_i^B, \frac{\partial u_i}{\partial t}\right), \tag{3.27}$$

the required result is obtained by the similar approaches used in the proof of Theorem 3.1. □

Finally, we consider the mixed weak form of the transformed Cahn–Hilliard equation with the Neumann–Dirichlet type boundary conditions as for $i = 1, \ldots, N$,

$$\left(\frac{\partial u_i}{\partial t}, \psi\right) + (\nabla \cdot \boldsymbol{w}_i, \psi) = 0, \tag{3.28a}$$

$$\left(\mathcal{M}(\mathbf{n})^{-1}\boldsymbol{w}_i, \boldsymbol{\omega}\right) = (q_i, \nabla \cdot \boldsymbol{\omega}), \tag{3.28b}$$

$$\lambda_i (\nabla \cdot \boldsymbol{s}_i, \varphi) + \left(\mathbf{v}_i^T \boldsymbol{\mu}^0(\mathbf{n}), \varphi\right) = \left(q_i + q_i^B, \varphi\right), \tag{3.28c}$$

$$(\boldsymbol{s}_i, \boldsymbol{\phi}) = (u_i, \nabla \cdot \boldsymbol{\phi}), \tag{3.28d}$$

where $\psi, \varphi \in L^2(\Omega)$, $\boldsymbol{\omega} \in H(\Omega; \mathrm{div})$ and $\boldsymbol{\phi} \in H_0(\Omega; \mathrm{div})$.

Theorem 3.4. *For the case of Neumann–Dirichlet type boundary conditions, the grand potential is decreased with the time and satisfies*

$$\frac{\partial G}{\partial t} = -\sum_{i=1}^{N} \|\mathcal{M}(\mathbf{n})^{-1/2}\boldsymbol{w}_i\|^2. \tag{3.29}$$

Proof. The proof is a combination of the proofs of Theorems 3.1 and 3.3. □

4. Unconditionally energy/potential stable semi-implicit time schemes

In this section, we will study the time discretization of the mixed forms stated in the previous section. Let the total time interval $I = (0, T_f]$, where $T_f > 0$. Divide I into K subintervals $I_k = (t_k, t_{k+1}]$, where $t_0 = 0$ and $t_K = T_f$, and denote $\delta t_k = t_{k+1} - t_k$. For any scalar $v(t)$ or vector $\mathbf{u}(t)$, we denote by v^k or $\mathbf{u}^k$ its approximation at the time t_k.

We now design an efficient energy/potential stable time marching scheme for two-phase interface models stated in the previous section. First of all, the implicit time scheme can be easy to be implemented for the linear terms in these transformed models. Moreover, this implicit treatment weakens the time step restriction and it is independent of any spatial discretization schemes. The main challenge arises from the nonlinear term $\boldsymbol{\mu}^0$, which has strong nonlinearity and fully coupling relation between all component molar densities. Although fully explicit time marching schemes for the nonlinear term $\boldsymbol{\mu}^0$ can reduce the nonlinearity and makes the whole system of equations easy to be solved, the stability demands a time step to be really tiny so that the resultant computation is extremely time consuming. On the other hand, the fully implicit time marching scheme for $\boldsymbol{\mu}^0$ is also not a perfect choice because in this case, all component molar density variables need to be solved by a fully coupled way, and the computation cost will become more expensive as the number of components becomes large.

Let us define $\widetilde{\mathbf{u}}_0^{k+1} = \mathbf{u}^k$ and $\widetilde{\mathbf{u}}_i^{k+1} = \left(u_1^{k+1}, \ldots, u_i^{k+1}, u_{i+1}^k, \ldots, u_N^k\right)^T$ for $1 \le i \le N$. It is apparent that $\mathbf{u}^{k+1} = \widetilde{\mathbf{u}}_N^{k+1}$. We now introduce the following semi-implicit time scheme for the mixed weak form of the transformed Cahn–Hilliard equation with the Neumann–Neumann type boundary conditions as

$$\left(\frac{u_i^{k+1} - u_i^k}{\delta t_k}, \psi\right) + \left(\nabla \cdot \boldsymbol{w}_i^{k+1}, \psi\right) = 0, \tag{4.1a}$$

$$\left(\mathcal{M}(\mathbf{n}^k)\boldsymbol{w}_i^{k+1}, \boldsymbol{\omega}\right) = (q_i^{k+1}, \nabla \cdot \boldsymbol{\omega}), \tag{4.1b}$$

$$\lambda_i \left(\nabla \cdot \boldsymbol{s}_i^{k+1}, \varphi\right) + \left(\frac{g_0(\widetilde{\mathbf{u}}_i^{k+1}) - g_0(\widetilde{\mathbf{u}}_{i-1}^{k+1})}{u_i^{k+1} - u_i^k}, \varphi\right) = \left(q_i^{k+1}, \varphi\right), \tag{4.1c}$$

$$\left(\boldsymbol{s}_i^{k+1}, \boldsymbol{\phi}\right) = (u_i^{k+1}, \nabla \cdot \boldsymbol{\phi}), \tag{4.1d}$$

where $i = 1, \ldots, N$ and $k = 0, \ldots, K-1$. Correspondingly, define the discrete Helmholtz free energy at the time t_k as

$$F^k = \int_\Omega \left(g_0(\mathbf{u}^k) + \frac{1}{2}\sum_{i=1}^N \lambda_i |\boldsymbol{s}_i^k|^2\right) d\mathbf{x}. \tag{4.2}$$

One advantage of the scheme given by (4.1) is that the coupling relation between the components is weakened in a semi-implicit approach, and thus we only solve separately N Cahn–Hilliard equations by a decoupled way.

Theorem 4.1. *For the Neumann–Neumann type boundary conditions, the semi-implicit time scheme (4.1) is unconditionally energy stable and the discrete Helmholtz free energies satisfy*

$$F^{k+1} - F^k + \frac{1}{2}\sum_{i=1}^N \lambda_i \|\boldsymbol{s}_i^{k+1} - \boldsymbol{s}_i^k\|^2 = -\delta t_k \sum_{i=1}^N \|\mathcal{M}(\mathbf{n}^k)^{-1/2}\boldsymbol{w}_i^{k+1}\|^2. \tag{4.3}$$

Proof. Firstly, we take $\psi = \delta t_k q_i^{k+1}$ in (4.1a) and $\boldsymbol{\omega} = \boldsymbol{w}_i^{k+1}$ in (4.1b), respectively, and obtain

$$\left(u_i^{k+1} - u_i^k, q_i^{k+1}\right) + \delta t_k \left(\nabla \cdot \boldsymbol{w}_i^{k+1}, q_i^{k+1}\right) = 0, \tag{4.4}$$

$$\|\mathcal{M}(\mathbf{n}^k)^{-1/2}\boldsymbol{w}_i^{k+1}\|^2 = (q_i^{k+1}, \nabla \cdot \boldsymbol{w}_i^{k+1}), \tag{4.5}$$

where $i = 1, \ldots, N$. Substituting (4.5) into (4.4) gives

$$\left(u_i^{k+1} - u_i^k, q_i^{k+1}\right) + \delta t_k \|\mathcal{M}(\mathbf{n}^k)^{-1/2}\boldsymbol{w}_i^{k+1}\|^2 = 0. \tag{4.6}$$

Choose $\varphi = \left(u_i^{k+1} - u_i^k\right)$ in (4.1c) to get

$$\lambda_i \left(\nabla \cdot \boldsymbol{s}_i^{k+1}, u_i^{k+1} - u_i^k\right) + \left(g_0(\widetilde{\mathbf{u}}_i^{k+1}) - g_0(\widetilde{\mathbf{u}}_{i-1}^{k+1}), 1\right) = \left(q_i^{k+1}, u_i^{k+1} - u_i^k\right). \tag{4.7}$$

Taking $\boldsymbol{\phi} = \boldsymbol{s}_i^{k+1}$ in (4.1d), we have

$$\|\boldsymbol{s}_i^{k+1}\|^2 = \left(u_i^{k+1}, \nabla \cdot \boldsymbol{s}_i^{k+1}\right). \tag{4.8}$$

Furthermore, it is followed from (4.8) that

$$\|\boldsymbol{s}_i^{k+1}\|^2 - \|\boldsymbol{s}_i^k\|^2 = \left(u_i^{k+1} - u_i^k, \nabla \cdot \boldsymbol{s}_i^{k+1}\right) + \left(u_i^k, \nabla \cdot \left(\boldsymbol{s}_i^{k+1} - \boldsymbol{s}_i^k\right)\right). \tag{4.9}$$

On the other hand, we can also take $\boldsymbol{\phi} = \left(\boldsymbol{s}_i^{k+1} - \boldsymbol{s}_i^k\right)$ in (4.1d)

$$\left(\boldsymbol{s}_i^{k+1}, \boldsymbol{s}_i^{k+1} - \boldsymbol{s}_i^k\right) = \left(u_i^{k+1}, \nabla \cdot \left(\boldsymbol{s}_i^{k+1} - \boldsymbol{s}_i^k\right)\right), \tag{4.10}$$

which is rewritten as

$$\frac{1}{2}\left(\|\boldsymbol{s}_i^{k+1}\|^2-\|\boldsymbol{s}_i^{k}\|^2+\|\boldsymbol{s}_i^{k+1}-\boldsymbol{s}_i^{k}\|^2\right)=\left(u_i^{k+1},\nabla\cdot\left(\boldsymbol{s}_i^{k+1}-\boldsymbol{s}_i^{k}\right)\right). \tag{4.11}$$

For kth time step, the choice $\boldsymbol{\phi}=\left(\boldsymbol{s}_i^{k+1}-\boldsymbol{s}_i^{k}\right)$ in (4.1d) gives

$$\left(\boldsymbol{s}_i^{k},\boldsymbol{s}_i^{k+1}-\boldsymbol{s}_i^{k}\right)=\left(u_i^{k},\nabla\cdot\left(\boldsymbol{s}_i^{k+1}-\boldsymbol{s}_i^{k}\right)\right). \tag{4.12}$$

It is derived from (4.10) and (4.12) that

$$\|\boldsymbol{s}_i^{k+1}-\boldsymbol{s}_i^{k}\|^2=\left(u_i^{k+1}-u_i^{k},\nabla\cdot\left(\boldsymbol{s}_i^{k+1}-\boldsymbol{s}_i^{k}\right)\right). \tag{4.13}$$

From (4.9), (4.11) and (4.13), we deduce

$$\frac{1}{2}\left(\|\boldsymbol{s}_i^{k+1}\|^2-\|\boldsymbol{s}_i^{k}\|^2+\|\boldsymbol{s}_i^{k+1}-\boldsymbol{s}_i^{k}\|^2\right)=\left(u_i^{k+1}-u_i^{k},\nabla\cdot\boldsymbol{s}_i^{k+1}\right). \tag{4.14}$$

Thus, we combine (4.6), (4.7) and (4.14) and find

$$\frac{1}{2}\lambda_i\left(\|\boldsymbol{s}_i^{k+1}\|^2-\|\boldsymbol{s}_i^{k}\|^2+\|\boldsymbol{s}_i^{k+1}-\boldsymbol{s}_i^{k}\|^2\right)+\left(g_0(\widetilde{\mathbf{u}}_i^{k+1})-g_0(\widetilde{\mathbf{u}}_{i-1}^{k+1}),1\right)=-\delta t_k\|\mathcal{M}(\mathbf{n}^k)^{-1/2}\boldsymbol{w}_i^{k+1}\|^2. \tag{4.15}$$

Eq. (4.3) is obtained by summing up (4.15) from $i=1$ to N and taking into account

$$\sum_{i=1}^{N}\left(g_0(\widetilde{\mathbf{u}}_i^{k+1})-g_0(\widetilde{\mathbf{u}}_{i-1}^{k+1}),1\right)=\left(g_0(\mathbf{u}^{k+1})-g_0(\mathbf{u}^{k}),1\right). \tag{4.16}$$

We claim that $F^{k+1}\le F^k$ as a direct result of (4.3). □

Similar to the scheme given by (4.1) for the Neumann–Neumann type boundary conditions, we now discuss the problems with the other boundary conditions. The semi-implicit time scheme for the mixed weak form of the transformed Cahn–Hilliard equation with the Dirichlet–Neumann type boundary conditions is described as

$$\left(\frac{u_i^{k+1}-u_i^{k}}{\delta t_k},\psi\right)+\left(\nabla\cdot\boldsymbol{w}_i^{k+1},\psi\right)=0, \tag{4.17a}$$

$$\left(\mathcal{M}(\mathbf{n}^k)^{-1}\boldsymbol{w}_i^{k+1},\boldsymbol{\omega}\right)=(q_i^{k+1},\nabla\cdot\boldsymbol{\omega}), \tag{4.17b}$$

$$\lambda_i\left(\nabla\cdot\boldsymbol{s}_i^{k+1},\varphi\right)+\left(\frac{g_0(\widetilde{\mathbf{u}}_i^{k+1})-g_0(\widetilde{\mathbf{u}}_{i-1}^{k+1})}{u_i^{k+1}-u_i^{k}},\varphi\right)=\left(q_i^{k+1},\varphi\right), \tag{4.17c}$$

$$\left(\boldsymbol{s}_i^{k+1},\boldsymbol{\phi}\right)=(u_i^{k+1},\nabla\cdot\boldsymbol{\phi})-\left(u_i^{B},\boldsymbol{\phi}\cdot\boldsymbol{\nu}_{\partial\Omega}\right)_{\partial\Omega}, \tag{4.17d}$$

where $i=1,\ldots,N$. The discrete Helmholtz free energy is defined as in (4.2).

Theorem 4.2. *For the Dirichlet–Neumann type boundary conditions, the semi-implicit time scheme (4.17) is unconditionally energy stable and the discrete Helmholtz free energies satisfy*

$$F^{k+1}-F^{k}+\frac{1}{2}\sum_{i=1}^{N}\lambda_i\|\boldsymbol{s}_i^{k+1}-\boldsymbol{s}_i^{k}\|^2=-\delta t_k\sum_{i=1}^{N}\|\mathcal{M}(\mathbf{n}^k)^{-1/2}\boldsymbol{w}_i^{k+1}\|^2. \tag{4.18}$$

Proof. It is similar to the proof of Theorem 4.1 that we have (4.4)–(4.7). By taking $\boldsymbol{\phi}=\boldsymbol{s}_i^{k+1}$ in (4.17d), we get

$$\|\boldsymbol{s}_i^{k+1}\|^2=\left(u_i^{k+1},\nabla\cdot\boldsymbol{s}_i^{k+1}\right)-\left(u_i^{B},\boldsymbol{s}_i^{k+1}\cdot\boldsymbol{\nu}_{\partial\Omega}\right)_{\partial\Omega}, \tag{4.19}$$

and furthermore

$$\|\boldsymbol{s}_i^{k+1}\|^2-\|\boldsymbol{s}_i^{k}\|^2=\left(u_i^{k+1}-u_i^{k},\nabla\cdot\boldsymbol{s}_i^{k+1}\right)+\left(u_i^{k},\nabla\cdot\left(\boldsymbol{s}_i^{k+1}-\boldsymbol{s}_i^{k}\right)\right)-\left(u_i^{B},\left(\boldsymbol{s}_i^{k+1}-\boldsymbol{s}_i^{k}\right)\cdot\boldsymbol{\nu}_{\partial\Omega}\right)_{\partial\Omega}. \tag{4.20}$$

On the other hand, we choose another test function $\boldsymbol{\phi}=\left(\boldsymbol{s}_i^{k+1}-\boldsymbol{s}_i^{k}\right)$ in (4.17d) and obtain that for $k+1$ time step

$$\left(\boldsymbol{s}_i^{k+1},\boldsymbol{s}_i^{k+1}-\boldsymbol{s}_i^{k}\right)=\left(u_i^{k+1},\nabla\cdot\left(\boldsymbol{s}_i^{k+1}-\boldsymbol{s}_i^{k}\right)\right)-\left(u_i^{B},\left(\boldsymbol{s}_i^{k+1}-\boldsymbol{s}_i^{k}\right)\cdot\boldsymbol{\nu}_{\partial\Omega}\right)_{\partial\Omega}, \tag{4.21}$$

and for k time step

$$\left(\boldsymbol{s}_i^{k},\boldsymbol{s}_i^{k+1}-\boldsymbol{s}_i^{k}\right)=\left(u_i^{k},\nabla\cdot\left(\boldsymbol{s}_i^{k+1}-\boldsymbol{s}_i^{k}\right)\right)-\left(u_i^{B},\left(\boldsymbol{s}_i^{k+1}-\boldsymbol{s}_i^{k}\right)\cdot\boldsymbol{\nu}_{\partial\Omega}\right)_{\partial\Omega}. \tag{4.22}$$

Thus, we get

$$\|\boldsymbol{s}_i^{k+1} - \boldsymbol{s}_i^k\|^2 = \left(u_i^{k+1} - u_i^k, \nabla \cdot \left(\boldsymbol{s}_i^{k+1} - \boldsymbol{s}_i^k\right)\right). \tag{4.23}$$

Noticing that

$$\left(\boldsymbol{s}_i^{k+1}, \boldsymbol{s}_i^{k+1} - \boldsymbol{s}_i^k\right) = \frac{1}{2}\left(\|\boldsymbol{s}_i^{k+1}\|^2 - \|\boldsymbol{s}_i^k\|^2 + \|\boldsymbol{s}_i^{k+1} - \boldsymbol{s}_i^k\|^2\right), \tag{4.24}$$

we reach that

$$\frac{1}{2}\left(\|\boldsymbol{s}_i^{k+1}\|^2 - \|\boldsymbol{s}_i^k\|^2 + \|\boldsymbol{s}_i^{k+1} - \boldsymbol{s}_i^k\|^2\right) = \left(u_i^{k+1} - u_i^k, \nabla \cdot \boldsymbol{s}_i^{k+1}\right). \tag{4.25}$$

The rest of the proof is the same to Theorem 4.1. □

For the Dirichlet–Dirichlet and Neumann–Dirichlet type boundary conditions, we define the discrete grand potential as

$$G^k = \int_\Omega \left(g_0(\mathbf{u}^k) - \sum_{i=1}^N q_i^B u_i^k + \frac{1}{2}\sum_{i=1}^N \lambda_i |\boldsymbol{s}_i^k|^2\right) d\mathbf{x}. \tag{4.26}$$

The mixed semi-implicit time scheme for the transformed Cahn–Hilliard equation with the Dirichlet–Dirichlet type boundary conditions is expressed as

$$\left(\frac{u_i^{k+1} - u_i^k}{\delta t_k}, \psi\right) + \left(\nabla \cdot \boldsymbol{w}_i^{k+1}, \psi\right) = 0, \tag{4.27a}$$

$$\left(\mathcal{M}(\mathbf{n}^k)^{-1}\boldsymbol{w}_i^{k+1}, \boldsymbol{\omega}\right) = (q_i^{k+1}, \nabla \cdot \boldsymbol{\omega}), \tag{4.27b}$$

$$\lambda_i\left(\nabla \cdot \boldsymbol{s}_i^{k+1}, \varphi\right) + \left(\frac{g_0(\widetilde{\mathbf{u}}_i^{k+1}) - g_0(\widetilde{\mathbf{u}}_{i-1}^{k+1})}{u_i^{k+1} - u_i^k}, \varphi\right) = \left(q_i^{k+1} + q_i^B, \varphi\right), \tag{4.27c}$$

$$\left(\boldsymbol{s}_i^{k+1}, \boldsymbol{\phi}\right) = (u_i^{k+1}, \nabla \cdot \boldsymbol{\phi}) - \left(u_i^B, \boldsymbol{\phi} \cdot \boldsymbol{\nu}_{\partial\Omega}\right)_{\partial\Omega}, \tag{4.27d}$$

where $i = 1, \ldots, N$.

Theorem 4.3. *For the Dirichlet–Dirichlet type boundary conditions, the semi-implicit time scheme (4.27) is unconditionally potential stable and the discrete grand potentials satisfy*

$$G^{k+1} - G^k + \frac{1}{2}\sum_{i=1}^N \lambda_i \|\boldsymbol{s}_i^{k+1} - \boldsymbol{s}_i^k\|^2 = -\delta t_k \sum_{i=1}^N \|\mathcal{M}(\mathbf{n}^k)^{-1/2}\boldsymbol{w}_i^{k+1}\|^2. \tag{4.28}$$

Proof. We consider only the differences from the proof of Theorem 4.1. For $1 \le i \le N$, taking $\varphi = \left(u_i^{k+1} - u_i^k\right)$ in (4.27c) leads to

$$\lambda_i\left(\nabla \cdot \boldsymbol{s}_i^{k+1}, u_i^{k+1} - u_i^k\right) + \left(g_0(\widetilde{\mathbf{u}}_i^{k+1}) - g_0(\widetilde{\mathbf{u}}_{i-1}^{k+1}), 1\right) - \left(q_i^B, u_i^{k+1} - u_i^k\right) = \left(q_i^{k+1}, u_i^{k+1} - u_i^k\right). \tag{4.29}$$

Similar to the proof of Theorem 4.1, we can arrive at

$$\begin{aligned}&\frac{1}{2}\lambda_i\left(\|\boldsymbol{s}_i^{k+1}\|^2 - \|\boldsymbol{s}_i^k\|^2 + \|\boldsymbol{s}_i^{k+1} - \boldsymbol{s}_i^k\|^2\right) + \left(g_0(\widetilde{\mathbf{u}}_i^{k+1}) - g_0(\widetilde{\mathbf{u}}_{i-1}^{k+1}), 1\right)\\ &\quad - \left(q_i^B, u_i^{k+1} - u_i^k\right) = -\delta t_k \|\mathcal{M}(\mathbf{n}^k)^{-1/2}\boldsymbol{w}_i^{k+1}\|^2.\end{aligned} \tag{4.30}$$

With the definition of the discrete grand potential, Eq. (4.28) is derived by the similar approaches used in the proof of Theorem 4.1. □

Finally, we consider the mixed semi-implicit time scheme for the transformed Cahn–Hilliard equation with the Neumann–Dirichlet type boundary conditions, which is given by

$$\left(\frac{u_i^{k+1} - u_i^k}{\delta t_k}, \psi\right) + \left(\nabla \cdot \boldsymbol{w}_i^{k+1}, \psi\right) = 0, \tag{4.31a}$$

$$\left(\mathcal{M}(\mathbf{n}^k)^{-1}\boldsymbol{w}_i^{k+1}, \boldsymbol{\omega}\right) = (q_i^{k+1}, \nabla \cdot \boldsymbol{\omega}), \tag{4.31b}$$

$$\lambda_i\left(\nabla \cdot \boldsymbol{s}_i^{k+1}, \varphi\right) + \left(\frac{g_0(\widetilde{\mathbf{u}}_i^{k+1}) - g_0(\widetilde{\mathbf{u}}_{i-1}^{k+1})}{u_i^{k+1} - u_i^k}, \varphi\right) = \left(q_i^{k+1} + q_i^B, \varphi\right), \tag{4.31c}$$

$$\left(\boldsymbol{s}_i^{k+1}, \boldsymbol{\phi}\right) = (u_i^{k+1}, \nabla \cdot \boldsymbol{\phi}), \tag{4.31d}$$

where $i = 1, \ldots, N$.

Theorem 4.4. *For the Neumann–Dirichlet type boundary conditions, the semi-implicit time scheme (4.31) is unconditionally potential stable and the discrete grand potentials satisfy*

$$G^{k+1} - G^k + \frac{1}{2}\sum_{i=1}^{N}\lambda_i\|\boldsymbol{s}_i^{k+1} - \boldsymbol{s}_i^k\|^2 = -\delta t_k \sum_{i=1}^{N}\|\mathcal{M}(\mathbf{n}^k)^{-1/2}\boldsymbol{w}_i^{k+1}\|^2. \tag{4.32}$$

Proof. The proof can be carried out by the similar approaches used in the proofs of Theorems 4.1 and 4.3. □

5. Mixed finite element approximations

The Mixed Finite Element (MFE) methods [39–41] have been used frequently in reservoir engineering problems for the reasons that they are capable to achieve very accurate and stable approximations of both the primary unknown and its flux across grid-cell interfaces. The MFE methods have the local mass conservation property, which is required for Neumann–Neumann and Dirichlet–Neumann boundary problems considered in this paper. In this work, the Raviart–Thomas mixed finite element method [40,42,43] will be used as the spatial discretization scheme.

5.1. Formulae of mixed finite element approximations

Let $\mathcal{E}_h$ be a quasi-uniform regular mesh of Ω. Let the approximating subspace duality $\mathbf{V}_r(\mathcal{E}_h) \subset V = H(\Omega; \mathrm{div})$ and $W_r(\mathcal{E}_h) \subset W = L^2(\Omega)$ be the r-th order ($r \geq 0$) Raviart–Thomas space (RT_r) on the partition $\mathcal{E}_h$.

For sake of simplicity, we consider only the mixed finite element approximation applied to the transformed Cahn–Hilliard equation with the Neumann–Neumann type boundary conditions, but the cases with the other three types of boundary conditions can be formulated by the similar routines. The continuous-in-time scheme can be formulated as: to seek for $U_i(\cdot, t), Q_i(\cdot, t) \in W_r(\mathcal{E}_h)$ and $\boldsymbol{W}_i(\cdot, t), \boldsymbol{S}_i(\cdot, t) \in \mathbf{V}_r(\mathcal{E}_h)$ such that the following equations hold for $t \in (0, T_f]$ and $i = 1, \ldots, N$:

$$\left(\frac{\partial U_i}{\partial t}, \psi\right) + (\nabla \cdot \boldsymbol{W}_i, \psi) = 0, \tag{5.1a}$$

$$\left(\mathcal{M}(\mathbb{Q}\mathbf{U})^{-1}\boldsymbol{W}_i, \boldsymbol{\omega}\right) = (Q_i, \nabla \cdot \boldsymbol{\omega}), \tag{5.1b}$$

$$\lambda_i\left(\nabla \cdot \boldsymbol{S}_i, \varphi\right) + \left(\mathbf{v}_i^T\boldsymbol{\mu}^0(\mathbf{n}_h), \varphi\right) = \left(Q_i, \varphi\right), \tag{5.1c}$$

$$(\boldsymbol{S}_i, \boldsymbol{\phi}) = (U_i, \nabla \cdot \boldsymbol{\phi}), \tag{5.1d}$$

where $\mathbf{U} = (U_1, \ldots, U_N)^T$, $\mathbf{n}_h = \mathbb{Q}\mathbf{U}$, $\psi, \varphi \in W_r$ and $\boldsymbol{\omega}, \boldsymbol{\phi} \in \mathbf{V}_r$.

Denote the approximations of $\mathbf{U}$ and $\mathbf{n}_h$ at the time t_k by $\mathbf{U}^k = \left(U_1^k, \ldots, U_N^k\right)^T$ and $\mathbf{n}_h^k = \mathbb{Q}\mathbf{U}^k$. Define $\widetilde{\mathbf{U}}_0^{k+1} = \mathbf{U}^k$ and $\widetilde{\mathbf{U}}_i^{k+1} = \left(U_1^{k+1}, \ldots, U_i^{k+1}, U_{i+1}^k, \ldots, U_N^k\right)^T$ for $1 \leq i \leq N$. We apply the semi-implicit time scheme stated in the previous section to (5.1) and then obtain the fully discrete formulation: to seek for $U_i^{k+1}, Q_i^{k+1} \in W_r(\mathcal{E}_h)$ and $\boldsymbol{W}_i^{k+1}, \boldsymbol{S}_i^{k+1} \in \mathbf{V}_r(\mathcal{E}_h)$ such that the following equations hold for $k = 0, \ldots, K-1$ and $i = 1, \ldots, N$:

$$\left(\frac{U_i^{k+1} - U_i^k}{\delta t_k}, \psi\right) + \left(\nabla \cdot \boldsymbol{W}_i^{k+1}, \psi\right) = 0, \tag{5.2a}$$

$$\left(\mathcal{M}(\mathbb{Q}\mathbf{U}^k)^{-1}\boldsymbol{W}_i^{k+1}, \boldsymbol{\omega}\right) = (Q_i^{k+1}, \nabla \cdot \boldsymbol{\omega}), \tag{5.2b}$$

$$\lambda_i\left(\nabla \cdot \boldsymbol{S}_i^{k+1}, \varphi\right) + \left(\frac{g_0(\widetilde{\mathbf{U}}_i^{k+1}) - g_0(\widetilde{\mathbf{U}}_{i-1}^{k+1})}{U_i^{k+1} - U_i^k}, \varphi\right) = \left(Q_i^{k+1}, \varphi\right), \tag{5.2c}$$

$$\left(\boldsymbol{S}_i^{k+1}, \boldsymbol{\phi}\right) = (U_i^{k+1}, \nabla \cdot \boldsymbol{\phi}), \tag{5.2d}$$

where $\psi, \varphi \in W_r$ and $\boldsymbol{\omega}, \boldsymbol{\phi} \in \mathbf{V}_r$.

It is noted that the stability property for the above mixed finite element approximations can also be proven by the similar approaches used in the previous sections.

5.2. Error estimates

In this subsection, we will estimate the approximate errors of mixed finite element discretization formulations given in (5.1) and (5.2). In what follows, we use C to indicate a generic positive constant independent of mesh size and time step size, but the values of C are probably different in different occurrences.

Denote by h the mesh size and $h \le h_0 (h_0 > 0)$. Furthermore, denote by r the order of Raviart–Thomas spaces. Let P_h be L^2-projection operator of W onto $W_h = W_r(\mathcal{E}_h)$, i.e., for $p \in W$, there exists a unique $P_h p \in W_h$ such that

$$(p - P_h p, w) = 0, \quad \forall w \in W_h. \tag{5.3}$$

Moreover, P_h satisfies the following approximation property

$$\|P_h p - p\| \le C \|p\|_{H^j(\Omega)} h^j, \quad 0 \le j \le r + 1. \tag{5.4}$$

Let $\Pi_h : V \to V_h$ denote the usual Raviart–Thomas projection, which has the following properties [40,42,43]

$$(\nabla \cdot (\mathbf{u} - \Pi_h \mathbf{u}), w) = 0, \quad w \in W_h, \tag{5.5}$$

$$\|\mathbf{u} - \Pi_h \mathbf{u}\| \le C \|\mathbf{u}\|_{(H^j(\Omega))^d} h^j, \quad 1 \le j \le r + 1, \tag{5.6}$$

$$\nabla \cdot \Pi_h = P_h \nabla. \tag{5.7}$$

For the continuous-in-time scheme, we define finite element solution errors as

$$E_{u_i} = u_i - U_i, \qquad E_{\boldsymbol{w}_i} = \boldsymbol{w}_i - \boldsymbol{W}_i, \qquad E_{\boldsymbol{s}_i} = \boldsymbol{s}_i - \boldsymbol{S}_i, \qquad E_{q_i} = q_i - Q_i.$$

Furthermore, define the interpolation errors as

$$E^I_{u_i} = P_h u_i - u_i, \qquad E^I_{\boldsymbol{w}_i} = \Pi_h \boldsymbol{w}_i - \boldsymbol{w}_i, \qquad E^I_{\boldsymbol{s}_i} = \Pi_h \boldsymbol{s}_i - \boldsymbol{s}_i, \qquad E^I_{q_i} = P_h q_i - q_i,$$

and also define the auxiliary errors as

$$E^A_{u_i} = P_h u_i - U_i, \qquad E^A_{\boldsymbol{w}_i} = \Pi_h \boldsymbol{w}_i - \boldsymbol{W}_i, \qquad E^A_{\boldsymbol{s}_i} = \Pi_h \boldsymbol{s}_i - \boldsymbol{S}_i, \qquad E^A_{q_i} = P_h q_i - Q_i.$$

For sake of simple and clear presentation of analysis techniques, we assume that $\mathcal{M} = 1$ in the following error analysis, but the proof can also be extended to the general case of $\mathcal{M}$. Moreover, we assume that the real and auxiliary exact solutions, including n_i, u_i, q_i, $\boldsymbol{w}_i$ and $\boldsymbol{s}_i$, are sufficiently smooth, and also assume that μ_i^0 $(1 \le i \le N)$ is Lipschitz continuous with respect to $\mathbf{n}$.

Theorem 5.1. *For given time $T > 0$, the solutions of (5.1) with $\mathcal{M} = 1$ satisfy the following error estimates*

$$\int_0^T \|E_{u_i}\|^2 dt + \left\| \int_0^T E_{q_i} dt \right\|^2 + \int_0^T \|E_{\boldsymbol{s}_i}\|^2 dt + \left\| \int_0^T E_{\boldsymbol{w}_i} dt \right\|^2 \le C h^{2\nu}, \tag{5.8}$$

$$\int_0^T \|n_i - n_{i,h}\|^2 dt \le C h^{2\nu}, \tag{5.9}$$

where $\nu = r + 1$, $1 \le i \le N$, and C is a positive constant depending on T and the exact solutions, but independent of h.

Proof. Firstly, it is observed that for $1 \le i \le N$,

$$\left(\frac{\partial E^A_{u_i}}{\partial t}, \psi \right) + \left(\nabla \cdot E^A_{\boldsymbol{w}_i}, \psi \right) = 0, \tag{5.10}$$

$$\left(E^A_{\boldsymbol{w}_i}, \boldsymbol{\omega} \right) = \left(E^A_{q_i}, \nabla \cdot \boldsymbol{\omega} \right) + \left(E^I_{\boldsymbol{w}_i}, \boldsymbol{\omega} \right), \tag{5.11}$$

$$\lambda_i \left(\nabla \cdot E^A_{\boldsymbol{s}_i}, \varphi \right) + \left(\mathbf{v}_i^T \left(\boldsymbol{\mu}^0(\mathbf{n}) - \boldsymbol{\mu}^0(\mathbf{n}_h) \right), \varphi \right) = \left(E^A_{q_i}, \varphi \right), \tag{5.12}$$

$$\left(E^A_{\boldsymbol{s}_i}, \boldsymbol{\phi} \right) = \left(E^A_{u_i}, \nabla \cdot \boldsymbol{\phi} \right) + \left(E^I_{\boldsymbol{s}_i}, \boldsymbol{\phi} \right), \tag{5.13}$$

where we have used the L^2 projection property, i.e., $\left(E^I_{q_i}, \nabla \cdot \boldsymbol{\omega} \right) = 0$, $\left(E^I_{u_i}, \psi \right) = 0$, $\left(E^I_{q_i}, \varphi \right) = 0$, and we have also used the Raviart–Thomas projection property, i.e., $\left(\nabla \cdot E^I_{\boldsymbol{w}_i}, \psi \right) = 0$ and $\left(\nabla \cdot E^I_{\boldsymbol{s}_i}, \varphi \right) = 0$. For $0 < t \le T$, integrating (5.10) in time from 0 to t and taking into account $E^A_{u_i} = 0$ at the initial time, we obtain

$$\left(E^A_{u_i}(t), \psi \right) + \left(\int_0^t \nabla \cdot E^A_{\boldsymbol{w}_i} ds, \psi \right) = 0. \tag{5.14}$$

By taking $\psi = E^A_{q_i}(t)$ in (5.14) and $\boldsymbol{\omega} = \int_0^t E^A_{\boldsymbol{w}_i} ds$ in (5.11), it follows that

$$\left(E^A_{u_i}(t), E^A_{q_i}(t) \right) + \left(\int_0^t \nabla \cdot E^A_{\boldsymbol{w}_i} ds, E^A_{q_i}(t) \right) = 0, \tag{5.15}$$

$$\left(E^A_{\boldsymbol{w}_i}(t), \int_0^t E^A_{\boldsymbol{w}_i} ds \right) = \left(E^A_{q_i}(t), \nabla \cdot \int_0^t E^A_{\boldsymbol{w}_i} ds \right) + \left(E^I_{\boldsymbol{w}_i}(t), \int_0^t E^A_{\boldsymbol{w}_i} ds \right). \tag{5.16}$$

Substituting (5.16) into (5.15) gives

$$\left(E^A_{u_i}(t), E^A_{q_i}(t)\right) + \left(E^A_{\boldsymbol{w}_i}(t), \int_0^t E^A_{\boldsymbol{w}_i} ds\right) = \left(E^I_{\boldsymbol{w}_i}(t), \int_0^t E^A_{\boldsymbol{w}_i} ds\right). \tag{5.17}$$

Taking $\varphi = E^A_{u_i}(t)$ in (5.12) leads to

$$\lambda_i \left(\nabla \cdot E^A_{\boldsymbol{s}_i}(t), E^A_{u_i}(t)\right) + \left(\mathbf{v}_i^T \left(\boldsymbol{\mu}^0(\mathbf{n}(t)) - \boldsymbol{\mu}^0(\mathbf{n}_h(t))\right), E^A_{u_i}(t)\right) = \left(E^A_{q_i}(t), E^A_{u_i}(t)\right). \tag{5.18}$$

Furthermore, take $\boldsymbol{\phi} = E^A_{\boldsymbol{s}_i}(t)$ in (5.13)

$$\|E^A_{\boldsymbol{s}_i}\|^2(t) = (E^A_{u_i}(t), \nabla \cdot E^A_{\boldsymbol{s}_i}(t)) + \left(E^I_{\boldsymbol{s}_i}(t), E^A_{\boldsymbol{s}_i}(t)\right). \tag{5.19}$$

Combine Eqs. (5.17)–(5.19) to get

$$\begin{aligned} &\lambda_i \|E^A_{\boldsymbol{s}_i}\|^2(t) + \left(E^A_{\boldsymbol{w}_i}(t), \int_0^t E^A_{\boldsymbol{w}_i} ds\right) \\ &= \left(E^I_{\boldsymbol{w}_i}(t), \int_0^t E^A_{\boldsymbol{w}_i} ds\right) + \lambda_i \left(E^I_{\boldsymbol{s}_i}(t), E^A_{\boldsymbol{s}_i}(t)\right) - \left(\mathbf{v}_i^T \left(\boldsymbol{\mu}^0(\mathbf{n}(t)) - \boldsymbol{\mu}^0(\mathbf{n}_h(t))\right), E^A_{u_i}(t)\right). \end{aligned} \tag{5.20}$$

For $0 < t' \le T$, integrate Eq. (5.20) in time t from 0 to t',

$$\begin{aligned} \lambda_i \int_0^{t'} \|E^A_{\boldsymbol{s}_i}\|^2 dt + \int_0^{t'} \left(E^A_{\boldsymbol{w}_i}(t), \int_0^t E^A_{\boldsymbol{w}_i} ds\right) dt &= \int_0^{t'} \left(E^I_{\boldsymbol{w}_i}(t), \int_0^t E^A_{\boldsymbol{w}_i} ds\right) dt + \lambda_i \int_0^{t'} \left(E^I_{\boldsymbol{s}_i}(t), E^A_{\boldsymbol{s}_i}(t)\right) dt \\ &+ \int_0^{t'} \left(\mathbf{v}_i^T \left(\boldsymbol{\mu}^0(\mathbf{n}_h(t)) - \boldsymbol{\mu}^0(\mathbf{n}(t))\right), E^A_{u_i}(t)\right) dt. \end{aligned} \tag{5.21}$$

Using the Lipschitz continuity of μ_i^0 and the Cauchy–Schwarz inequality, we estimate the terms in (5.21) as

$$\int_0^{t'} \left(E^A_{\boldsymbol{w}_i}(t), \int_0^t E^A_{\boldsymbol{w}_i} ds\right) dt = \frac{1}{2} \left\| \int_0^{t'} E^A_{\boldsymbol{w}_i} dt \right\|^2, \tag{5.22}$$

$$\int_0^{t'} \left(E^I_{\boldsymbol{w}_i}(t), \int_0^t E^A_{\boldsymbol{w}_i} ds\right) dt \le C_1 h^{2\nu} + \frac{1}{2} \int_0^{t'} \left\| \int_0^t E^A_{\boldsymbol{w}_i} ds \right\|^2 dt, \tag{5.23}$$

$$\lambda_i \int_0^{t'} \left(E^I_{\boldsymbol{s}_i}(t), E^A_{\boldsymbol{s}_i}(t)\right) dt \le C_2 h^{2\nu} + \frac{1}{2} \lambda_i \int_0^{t'} \|E^A_{\boldsymbol{s}_i}\|^2 dt, \tag{5.24}$$

$$\int_0^{t'} \left(\mathbf{v}_i^T \left(\boldsymbol{\mu}^0(\mathbf{n}_h(t)) - \boldsymbol{\mu}^0(\mathbf{n}(t))\right), E^A_{u_i}(t)\right) dt \le C_3 h^{2\nu} + \frac{1}{2} C_4 \sum_{i=1}^N \int_0^{t'} \|E^A_{u_i}\|^2 dt, \tag{5.25}$$

where $C_j (1 \le j \le 4)$ are positive constants depending on t' and the exact solutions, but independent of h. It is deduced from (5.21)–(5.25) that

$$\lambda_i \int_0^{t'} \|E^A_{\boldsymbol{s}_i}\|^2 dt + \left\| \int_0^{t'} E^A_{\boldsymbol{w}_i} dt \right\|^2 \le C_5 h^{2\nu} + \int_0^{t'} \left\| \int_0^t E^A_{\boldsymbol{w}_i} ds \right\|^2 dt + C_4 \sum_{i=1}^N \int_0^{t'} \|E^A_{u_i}\|^2 dt, \tag{5.26}$$

where $C_5 = 2(C_1 + C_2 + C_3)$. It is followed by applying Gronwall's lemma to (5.26) that

$$\lambda_i \int_0^{t'} \|E^A_{\boldsymbol{s}_i}\|^2 dt + \left\| \int_0^{t'} E^A_{\boldsymbol{w}_i} dt \right\|^2 \le \exp(t') \left(C_5 h^{2\nu} + C_4 \sum_{i=1}^N \int_0^{t'} \|E^A_{u_i}\|^2 dt \right). \tag{5.27}$$

On the other hand, taking $\psi = E^A_{u_i}(t)$ in (5.14), $\boldsymbol{\omega} = E^A_{\boldsymbol{s}_i}(t)$ in (5.11), $\varphi = \int_0^t E^A_{q_i} ds$ in (5.12) and $\boldsymbol{\phi} = \int_0^t E^A_{\boldsymbol{w}_i} ds$ in (5.13), we get

$$\|E^A_{u_i}\|^2(t) + \left(\int_0^t \nabla \cdot E^A_{\boldsymbol{w}_i} ds, E^A_{u_i}(t)\right) = 0, \tag{5.28}$$

$$\left(\int_0^t E^A_{\boldsymbol{w}_i} ds, E^A_{\boldsymbol{s}_i}(t)\right) = \left(\int_0^t E^A_{q_i} ds, \nabla \cdot E^A_{\boldsymbol{s}_i}(t)\right) + \left(\int_0^t E^I_{\boldsymbol{w}_i} ds, E^A_{\boldsymbol{s}_i}(t)\right), \tag{5.29}$$

$$\lambda_i\left(\nabla\cdot E^A_{\boldsymbol{s}_i}(t),\int_0^t E^A_{q_i}ds\right)+\left(\mathbf{v}_i^T\left(\boldsymbol{\mu}^0(\mathbf{n}(t))-\boldsymbol{\mu}^0(\mathbf{n}_h(t))\right),\int_0^t E^A_{q_i}ds\right)=\left(E^A_{q_i}(t),\int_0^t E^A_{q_i}ds\right),\tag{5.30}$$

$$\left(E^A_{\boldsymbol{s}_i}(t),\int_0^t E^A_{\boldsymbol{w}_i}ds\right)=\left(E^A_{u_i}(t),\int_0^t\nabla\cdot E^A_{\boldsymbol{w}_i}ds\right)+\left(E^I_{\boldsymbol{s}_i}(t),\int_0^t E^A_{\boldsymbol{w}_i}ds\right).\tag{5.31}$$

Combining Eqs. (5.28)–(5.31) gives

$$\begin{aligned}&\lambda_i\|E^A_{u_i}\|^2(t)+\left(E^A_{q_i}(t),\int_0^t E^A_{q_i}ds\right)=\lambda_i\left(E^I_{\boldsymbol{s}_i}(t),\int_0^t E^A_{\boldsymbol{w}_i}ds\right)\\&\quad-\lambda_i\left(\int_0^t E^I_{\boldsymbol{w}_i}ds,E^A_{\boldsymbol{s}_i}(t)\right)+\left(\mathbf{v}_i^T\left(\boldsymbol{\mu}^0(\mathbf{n}(t))-\boldsymbol{\mu}^0(\mathbf{n}_h(t))\right),\int_0^t E^A_{q_i}ds\right).\end{aligned}\tag{5.32}$$

Denote $\lambda_{\min}=\min_{1\le i\le N}\{\lambda_i\}$, and suppose that α_1,α_2 are given positive constants satisfying $\alpha_1\le\frac{1}{4N}\lambda_{\min}/(\exp(T)C_4)$ and $\alpha_2\le\frac{1}{4N}\lambda_{\min}$. Integrating Eq. (5.32) in time t from 0 to t', and then using the Lipschitz continuity of μ_i^0 and the Cauchy–Schwarz inequality, we obtain

$$\begin{aligned}&\lambda_i\int_0^{t'}\|E^A_{u_i}\|^2dt+\frac{1}{2}\left\|\int_0^{t'}E^A_{q_i}dt\right\|^2\\&\le C_6h^{2\nu}+\frac{\alpha_1}{2t'}\int_0^{t'}\left\|\int_0^t E^A_{\boldsymbol{w}_i}ds\right\|^2dt+\frac{1}{2}\alpha_1\lambda_i\int_0^{t'}\left\|E^A_{\boldsymbol{s}_i}\right\|^2dt+\alpha_2\sum_{i=1}^N\int_0^{t'}\|E^A_{u_i}\|^2dt+C_7\int_0^{t'}\left\|\int_0^t E^A_{q_i}ds\right\|^2dt\\&\le\left(C_6+\alpha_1\exp(t')C_5\right)h^{2\nu}+\left(\alpha_1\exp(t')C_4+\alpha_2\right)\sum_{i=1}^N\int_0^{t'}\|E^A_{u_i}\|^2dt+C_7\int_0^{t'}\left\|\int_0^t E^A_{q_i}ds\right\|^2dt,\end{aligned}\tag{5.33}$$

where we have also used the estimate (5.27). In (5.33), C_6 is a positive constant depending on α_1, t' and the exact solutions, and C_7 is a positive constant depending on α_2, but both constants are independent of h. Taking into account the choices of α_1 and α_2, we obtain from (5.33) that

$$\frac{1}{2}\lambda_{\min}\sum_{i=1}^N\int_0^{t'}\|E^A_{u_i}\|^2dt+\frac{1}{2}\sum_{i=1}^N\left\|\int_0^{t'}E^A_{q_i}dt\right\|^2\le C_8h^{2\nu}+C_7N\sum_{i=1}^N\int_0^{t'}\left\|\int_0^t E^A_{q_i}ds\right\|^2dt,\tag{5.34}$$

where $C_8=N\left(C_6+\alpha_1\exp(T)C_5\right)$. It is obtained by applying Gronwall's lemma to (5.34) that

$$\lambda_{\min}\sum_{i=1}^N\int_0^{t'}\|E^A_{u_i}\|^2dt+\sum_{i=1}^N\left\|\int_0^{t'}E^A_{q_i}dt\right\|^2\le C_9h^{2\nu},\tag{5.35}$$

and furthermore, substituting (5.35) into (5.27) yields

$$\lambda_i\int_0^{t'}\|E^A_{\boldsymbol{s}_i}\|^2dt+\left\|\int_0^{t'}E^A_{\boldsymbol{w}_i}dt\right\|^2\le C_{10}h^{2\nu},\tag{5.36}$$

where C_9 and C_{10} are independent of h. The required results are obtained by the triangle rule and the linear transformation. □

We now estimate the numerical errors of fully discrete formulations given by (5.2) with $\mathcal{M}=1$ and uniform time step sizes. The fully discrete errors are defined as

$$E^k_{u_i}=u_i(t_k)-U^k_i,\qquad E^k_{\boldsymbol{w}_i}=\boldsymbol{w}_i(t_k)-\boldsymbol{W}^k_i,\qquad E^k_{\boldsymbol{s}_i}=\boldsymbol{s}_i(t_k)-\boldsymbol{S}^k_i,\qquad E^k_{q_i}=q_i(t_k)-Q^k_i.$$

Moreover, we define the interpolation errors and the auxiliary errors as

$$\begin{aligned}&\chi^k_{u_i}=P_hu_i(t_k)-u_i(t_k),\qquad\chi^k_{\boldsymbol{w}_i}=\Pi_h\boldsymbol{w}_i(t_k)-\boldsymbol{w}_i(t_k),\qquad\chi^k_{\boldsymbol{s}_i}=\Pi_h\boldsymbol{s}_i(t_k)-\boldsymbol{s}_i(t_k),\\&\chi^k_{q_i}=P_hq_i(t_k)-q_i(t_k),\qquad\xi^k_{u_i}=P_hu_i(t_k)-U^k_i,\qquad\xi^k_{\boldsymbol{w}_i}=\Pi_h\boldsymbol{w}_i(t_k)-\boldsymbol{W}^k_i,\\&\xi^k_{\boldsymbol{s}_i}=\Pi_h\boldsymbol{s}_i(t_k)-\boldsymbol{S}^k_i,\qquad\xi^k_{q_i}=P_hq_i(t_k)-Q^k_i.\end{aligned}$$

Theorem 5.2. *For given time $T > 0$ and positive integer K, we determine the time step size $\delta t = T/K$. The solutions of (5.2) with $\mathcal{M} = 1$ satisfy the following error estimates*

$$\delta t \sum_{k=1}^{K} \|E_{u_i}^k\|^2 + \left\| \delta t \sum_{k=1}^{K} E_{q_i}^k \right\|^2 + \delta t \sum_{k=1}^{K} \left\|E_{\boldsymbol{s}_i}^k\right\|^2 + \left\| \delta t \sum_{k=1}^{K} E_{\boldsymbol{w}_i}^k \right\|^2 \leq C((\delta t)^2 + h^{2\nu}), \tag{5.37}$$

$$\delta t \sum_{k=1}^{K} \|n_i(t_k) - n_{i,h}^k\|^2 \leq C((\delta t)^2 + h^{2\nu}), \tag{5.38}$$

where $\nu = r + 1$, $1 \leq i \leq N$, and C is a positive constant depending on T and the exact solutions, but independent of h and δt.

Proof. For $1 \leq i \leq N$, using the L^2 projection property and Raviart–Thomas projection property, we obtain that

$$\left(\frac{\xi_{u_i}^{k+1} - \xi_{u_i}^k}{\delta t}, \psi\right) + \left(\nabla \cdot \xi_{\boldsymbol{w}_i}^{k+1}, \psi\right) = \left(\rho^{k+1}, \psi\right), \tag{5.39}$$

$$\left(\xi_{\boldsymbol{w}_i}^{k+1}, \boldsymbol{\omega}\right) = \left(\xi_{q_i}^{k+1}, \nabla \cdot \boldsymbol{\omega}\right) + \left(\chi_{\boldsymbol{w}_i}^{k+1}, \boldsymbol{\omega}\right), \tag{5.40}$$

$$\lambda_i \left(\nabla \cdot \xi_{\boldsymbol{s}_i}^{k+1}, \varphi\right) + \left(\pi^{k+1}, \varphi\right) = \left(\xi_{q_i}^{k+1}, \varphi\right), \tag{5.41}$$

$$\left(\xi_{\boldsymbol{s}_i}^{k+1}, \boldsymbol{\phi}\right) = \left(\xi_{u_i}^{k+1}, \nabla \cdot \boldsymbol{\phi}\right) + \left(\chi_{\boldsymbol{s}_i}^{k+1}, \boldsymbol{\phi}\right), \tag{5.42}$$

where

$$\rho^{k+1} = \frac{u_i(t_{k+1}) - u_i(t_k)}{\delta t} - \frac{\partial u_i}{\partial t}(t_{k+1}),$$

$$\pi^{k+1} = \mathbf{v}_i^T \boldsymbol{\mu}^0(\mathbf{n}(t_{k+1})) - \frac{g_0(\widetilde{\mathbf{U}}_i^{k+1}) - g_0(\widetilde{\mathbf{U}}_{i-1}^{k+1})}{U_i^{k+1} - U_i^k}.$$

Since $\xi_{u_i}^0 = 0$, it is deduced from (5.39) that

$$\left(\xi_{u_i}^{k+1}, \psi\right) + \delta t \left(\sum_{j=1}^{k+1} \nabla \cdot \xi_{\boldsymbol{w}_i}^j, \psi\right) = \delta t \left(\sum_{j=1}^{k+1} \rho^j, \psi\right), \tag{5.43}$$

and furthermore, we take $\psi = \xi_{q_i}^{k+1}$ to obtain

$$\left(\xi_{u_i}^{k+1}, \xi_{q_i}^{k+1}\right) + \delta t \left(\sum_{j=1}^{k+1} \nabla \cdot \xi_{\boldsymbol{w}_i}^j, \xi_{q_i}^{k+1}\right) = \delta t \left(\sum_{j=1}^{k+1} \rho^j, \xi_{q_i}^{k+1}\right). \tag{5.44}$$

Taking $\boldsymbol{\omega} = \sum_{j=1}^{k+1} \xi_{\boldsymbol{w}_i}^j$ in (5.40) yields

$$\left(\xi_{\boldsymbol{w}_i}^{k+1}, \sum_{j=1}^{k+1} \xi_{\boldsymbol{w}_i}^j\right) = \left(\xi_{q_i}^{k+1}, \sum_{j=1}^{k+1} \nabla \cdot \xi_{\boldsymbol{w}_i}^j\right) + \left(\chi_{\boldsymbol{w}_i}^{k+1}, \sum_{j=1}^{k+1} \xi_{\boldsymbol{w}_i}^j\right). \tag{5.45}$$

Substituting (5.45) into (5.44) gives

$$\left(\xi_{u_i}^{k+1}, \xi_{q_i}^{k+1}\right) + \delta t \left(\xi_{\boldsymbol{w}_i}^{k+1}, \sum_{j=1}^{k+1} \xi_{\boldsymbol{w}_i}^j\right) = \delta t \left(\sum_{j=1}^{k+1} \rho^j, \xi_{q_i}^{k+1}\right) + \delta t \left(\chi_{\boldsymbol{w}_i}^{k+1}, \sum_{j=1}^{k+1} \xi_{\boldsymbol{w}_i}^j\right). \tag{5.46}$$

Taking $\varphi = \xi_{u_i}^{k+1}$ in (5.41) and $\boldsymbol{\phi} = \xi_{\boldsymbol{s}_i}^{k+1}$ in (5.42) leads to

$$\lambda_i \left(\nabla \cdot \xi_{\boldsymbol{s}_i}^{k+1}, \xi_{u_i}^{k+1}\right) + \left(\pi^{k+1}, \xi_{u_i}^{k+1}\right) = \left(\xi_{q_i}^{k+1}, \xi_{u_i}^{k+1}\right), \tag{5.47}$$

$$\left\|\xi_{\boldsymbol{s}_i}^{k+1}\right\|^2 = \left(\xi_{u_i}^{k+1}, \nabla \cdot \xi_{\boldsymbol{s}_i}^{k+1}\right) + \left(\chi_{\boldsymbol{s}_i}^{k+1}, \xi_{\boldsymbol{s}_i}^{k+1}\right). \tag{5.48}$$

Combining Eqs. (5.46)–(5.48), we get

$$\lambda_i \left\|\xi_{\boldsymbol{s}_i}^{k+1}\right\|^2 + \delta t \left(\xi_{\boldsymbol{w}_i}^{k+1}, \sum_{j=1}^{k+1} \xi_{\boldsymbol{w}_i}^j\right) = \delta t \left(\sum_{j=1}^{k+1} \rho^j, \xi_{q_i}^{k+1}\right) + \delta t \left(\chi_{\boldsymbol{w}_i}^{k+1}, \sum_{j=1}^{k+1} \xi_{\boldsymbol{w}_i}^j\right) + \lambda_i \left(\chi_{\boldsymbol{s}_i}^{k+1}, \xi_{\boldsymbol{s}_i}^{k+1}\right) - \left(\pi^{k+1}, \xi_{u_i}^{k+1}\right). \tag{5.49}$$

For given integer $0 < k' \le K$, summing Eq. (5.49) yields

$$\lambda_i \delta t \sum_{k=1}^{k'} \left\| \xi_{\boldsymbol{s}_i}^k \right\|^2 + \delta t \sum_{k=1}^{k'} \left(\xi_{\boldsymbol{w}_i}^k, \delta t \sum_{j=1}^{k} \xi_{\boldsymbol{w}_i}^j \right) = \delta t \sum_{k=1}^{k'} \left(\delta t \sum_{j=1}^{k} \rho^j, \xi_{q_i}^k \right) + \delta t \sum_{k=1}^{k'} \left(\chi_{\boldsymbol{w}_i}^k, \delta t \sum_{j=1}^{k} \xi_{\boldsymbol{w}_i}^j \right) + \lambda_i \delta t \sum_{k=1}^{k'} \left(\chi_{\boldsymbol{s}_i}^k, \xi_{\boldsymbol{s}_i}^k \right) - \delta t \sum_{k=1}^{k'} \left(\pi^k, \xi_{u_i}^k \right). \tag{5.50}$$

Since Taylor's theorem gives

$$\|\rho^{k+1}\|^2 \le \frac{1}{3} \delta t \int_{t_k}^{t_{k+1}} \left\| \frac{\partial^2 u_i}{\partial t^2} \right\|^2 dt, \tag{5.51}$$

the first term on the right-hand side of (5.50) is estimated as

$$\begin{aligned} \delta t \sum_{k=1}^{k'} \left(\delta t \sum_{j=1}^{k} \rho^j, \xi_{q_i}^k \right) &= \left(\delta t \sum_{k=1}^{k'} \rho^k, \delta t \sum_{k=1}^{k'} \xi_{q_i}^k \right) + (\delta t)^2 \sum_{k=1}^{k'} \left(\rho^k, \xi_{q_i}^k \right) - \delta t \sum_{k=1}^{k'} \left(\rho^k, \delta t \sum_{j=1}^{k} \xi_{q_i}^j \right) \\ &\le \frac{1}{2} \left\| \delta t \sum_{k=1}^{k'} \rho^k \right\|^2 + \frac{1}{2} \left\| \delta t \sum_{k=1}^{k'} \xi_{q_i}^k \right\|^2 + \delta t \sum_{k=1}^{k'} \|\rho^k\|^2 \\ &\quad + \frac{1}{2} (\delta t)^3 \sum_{k=1}^{k'} \|\xi_{q_i}^k\|^2 + \frac{1}{2} \delta t \sum_{k=1}^{k'} \left\| \delta t \sum_{j=1}^{k} \xi_{q_i}^j \right\|^2 \\ &\le C_1 (\delta t)^2 + \frac{1}{2} \left\| \delta t \sum_{k=1}^{k'} \xi_{q_i}^k \right\|^2 + \frac{1}{2} \delta t \sum_{k=1}^{k'} \left\| \delta t \sum_{j=1}^{k} \xi_{q_i}^j \right\|^2, \end{aligned} \tag{5.52}$$

where we have also used the stability $\delta t \sum_{k=1}^{K} \|Q_i^k\|^2 + \delta t \sum_{k=1}^{K} \|P_h q_i(t_k)\|^2 \le C$ for some positive constant C independent of h and δt (that can be easily proved, so we omit the proof). Using the Lipschitz continuity of μ_i^0 and Cauchy–Schwarz inequality, we estimate the second and third terms on the right-hand side of (5.50) as

$$\delta t \sum_{k=1}^{k'} \left(\chi_{\boldsymbol{w}_i}^k, \delta t \sum_{j=1}^{k} \xi_{\boldsymbol{w}_i}^j \right) \le C_2 h^{2\nu} + \frac{1}{2} \delta t \sum_{k=1}^{k'} \left\| \delta t \sum_{j=1}^{k} \xi_{\boldsymbol{w}_i}^j \right\|^2, \tag{5.53}$$

$$\lambda_i \delta t \sum_{k=1}^{k'} \left(\chi_{\boldsymbol{s}_i}^k, \xi_{\boldsymbol{s}_i}^k \right) \le C_3 h^{2\nu} + \frac{1}{2} \lambda_i \delta t \sum_{k=1}^{k'} \left\| \xi_{\boldsymbol{s}_i}^k \right\|^2. \tag{5.54}$$

For π^{k+1}, we have the following estimate

$$\begin{aligned} \left\| \pi^{k+1} \right\| &\le \left\| \mathbf{v}_i^T \boldsymbol{\mu}^0(\mathbf{n}(t_{k+1})) - \mathbf{v}_i^T \boldsymbol{\mu}^0(\mathbb{Q}\widetilde{\mathbf{U}}_i^{k+1}) \right\| + \left\| \mathbf{v}_i^T \boldsymbol{\mu}^0(\mathbb{Q}\widetilde{\mathbf{U}}_i^{k+1}) - \frac{g_0(\widetilde{\mathbf{U}}_i^{k+1}) - g_0(\widetilde{\mathbf{U}}_{i-1}^{k+1})}{U_i^{k+1} - U_i^k} \right\| \\ &\le C_4 \delta t + C_5 h^{\nu} + C_6 \left(\sum_{j=1}^{i} \left\| \xi_{u_j}^{k+1} \right\| + \sum_{j=i+1}^{N} \left\| \xi_{u_j}^k \right\| \right). \end{aligned} \tag{5.55}$$

From this, the last term on the right-hand side of (5.50) is estimated as

$$-\delta t \sum_{k=1}^{k'} \left(\pi^k, \xi_{u_i}^k \right) \le C_7 (\delta t)^2 + C_8 h^{2\nu} + \frac{1}{2} C_9 \delta t \sum_{i=1}^{N} \sum_{k=1}^{k'} \left\| \xi_{u_i}^k \right\|^2. \tag{5.56}$$

Based on the above estimates, we obtain

$$\begin{aligned} \lambda_i \delta t \sum_{k=1}^{k'} \left\| \xi_{\boldsymbol{s}_i}^k \right\|^2 + \left\| \delta t \sum_{j=1}^{k'} \xi_{\boldsymbol{w}_i}^j \right\|^2 &\le C_{10} (\delta t)^2 + C_{11} h^{2\nu} + \delta t \sum_{k=1}^{k'} \left\| \delta t \sum_{j=1}^{k} \xi_{\boldsymbol{w}_i}^j \right\|^2 \\ &\quad + C_9 \delta t \sum_{i=1}^{N} \sum_{k=1}^{k'} \left\| \xi_{u_i}^k \right\|^2 + \left\| \delta t \sum_{k=1}^{k'} \xi_{q_i}^k \right\|^2 + \delta t \sum_{k=1}^{k'} \left\| \delta t \sum_{j=1}^{k} \xi_{q_i}^j \right\|^2, \end{aligned} \tag{5.57}$$

where we have also used the identity [44]

$$2\sum_{k=1}^{k'}\left(\xi_{\boldsymbol{w}_i}^{k},\sum_{j=1}^{k}\xi_{\boldsymbol{w}_i}^{j}\right)=\left\|\sum_{j=1}^{k'}\xi_{\boldsymbol{w}_i}^{j}\right\|^2+\sum_{j=1}^{k'}\left\|\xi_{\boldsymbol{w}_i}^{j}\right\|^2. \tag{5.58}$$

Applying discrete Gronwall's lemma to (5.57) leads to

$$\begin{aligned}\lambda_i\delta t\sum_{k=1}^{k'}\left\|\xi_{\boldsymbol{s}_i}^{k}\right\|^2+\left\|\delta t\sum_{k=1}^{k'}\xi_{\boldsymbol{w}_i}^{k}\right\|^2\le\exp(T)\Bigg(&C_{10}(\delta t)^2+C_{11}h^{2\nu}+C_9\delta t\sum_{i=1}^{N}\sum_{k=1}^{k'}\left\|\xi_{u_i}^{k}\right\|^2\\&+\left\|\delta t\sum_{k=1}^{k'}\xi_{q_i}^{k}\right\|^2+\delta t\sum_{k=1}^{k'}\left\|\delta t\sum_{j=1}^{k}\xi_{q_i}^{j}\right\|^2\Bigg),\end{aligned} \tag{5.59}$$

where C_j are positive constants, which may depend on T and the exact solutions, but independent of h and δt.

On the other hand, taking $\psi=\xi_{u_i}^{k+1}$ in (5.43), $\boldsymbol{\omega}=\xi_{\boldsymbol{s}_i}^{k+1}$ in (5.40), $\varphi=\sum_{j=1}^{k+1}\xi_{q_i}^{j}$ in (5.41) and $\boldsymbol{\phi}=\sum_{j=1}^{k+1}\xi_{\boldsymbol{w}_i}^{j}$ in (5.42), we get

$$\|\xi_{u_i}^{k+1}\|^2+\delta t\left(\sum_{j=1}^{k+1}\nabla\cdot\xi_{\boldsymbol{w}_i}^{j},\xi_{u_i}^{k+1}\right)=\left(\delta t\sum_{j=1}^{k+1}\rho^{j},\xi_{u_i}^{k+1}\right), \tag{5.60}$$

$$\left(\sum_{j=1}^{k+1}\xi_{\boldsymbol{w}_i}^{j},\xi_{\boldsymbol{s}_i}^{k+1}\right)=\left(\sum_{j=1}^{k+1}\xi_{q_i}^{j},\nabla\cdot\xi_{\boldsymbol{s}_i}^{k+1}\right)+\left(\sum_{j=1}^{k+1}\chi_{\boldsymbol{w}_i}^{j},\xi_{\boldsymbol{s}_i}^{k+1}\right), \tag{5.61}$$

$$\lambda_i\left(\nabla\cdot\xi_{\boldsymbol{s}_i}^{k+1},\sum_{j=1}^{k+1}\xi_{q_i}^{j}\right)+\left(\pi^{k+1},\sum_{j=1}^{k+1}\xi_{q_i}^{j}\right)=\left(\xi_{q_i}^{k+1},\sum_{j=1}^{k+1}\xi_{q_i}^{j}\right), \tag{5.62}$$

$$\left(\xi_{\boldsymbol{s}_i}^{k+1},\sum_{j=1}^{k+1}\xi_{\boldsymbol{w}_i}^{j}\right)=\left(\xi_{u_i}^{k+1},\sum_{j=1}^{k+1}\nabla\cdot\xi_{\boldsymbol{w}_i}^{j}\right)+\left(\chi_{\boldsymbol{s}_i}^{k+1},\sum_{j=1}^{k+1}\xi_{\boldsymbol{w}_i}^{j}\right). \tag{5.63}$$

The combination of Eqs. (5.60)–(5.63) gives

$$\begin{aligned}&\|\xi_{u_i}^{k+1}\|^2+\lambda_i^{-1}\delta t\left(\xi_{q_i}^{k+1},\sum_{j=1}^{k+1}\xi_{q_i}^{j}\right)=\left(\delta t\sum_{j=1}^{k+1}\rho^{j},\xi_{u_i}^{k+1}\right)\\&-\delta t\left(\sum_{j=1}^{k+1}\chi_{\boldsymbol{w}_i}^{j},\xi_{\boldsymbol{s}_i}^{k+1}\right)+\lambda_i^{-1}\delta t\left(\pi^{k+1},\sum_{j=1}^{k+1}\xi_{q_i}^{j}\right)+\delta t\left(\chi_{\boldsymbol{s}_i}^{k+1},\sum_{j=1}^{k+1}\xi_{\boldsymbol{w}_i}^{j}\right).\end{aligned} \tag{5.64}$$

Let α_1, α_2 be positive constants, then it is obtained by the similar techniques used to deduce (5.57) that

$$\begin{aligned}&\lambda_i\delta t\sum_{k=1}^{k'}\|\xi_{u_i}^{k}\|^2+\frac{1}{2}\left\|\delta t\sum_{k=1}^{k'}\xi_{q_i}^{k}\right\|^2\\&\le C_{12}(\delta t)^2+C_{13}h^{2\nu}+\frac{\alpha_1}{T}\delta t\sum_{k=1}^{k'}\left\|\delta t\sum_{j=1}^{k}\xi_{\boldsymbol{w}_i}^{j}\right\|^2+\alpha_1\delta t\lambda_i\sum_{k=1}^{k'}\|\xi_{\boldsymbol{s}_i}^{k}\|^2\\&\quad+\alpha_2\delta t\sum_{k=1}^{k'}\sum_{i=1}^{N}\|\xi_{u_i}^{k}\|^2+C_{14}\delta t\sum_{k=1}^{k'}\left\|\delta t\sum_{j=1}^{k}\xi_{q_i}^{j}\right\|^2\\&\le\left(2\alpha_1\exp(T)C_{10}+C_{12}\right)(\delta t)^2+\left(C_{13}+2\alpha_1\exp(T)C_{11}\right)h^{2\nu}\\&\quad+\left(2\alpha_1\exp(T)C_9+\alpha_2\right)\delta t\sum_{k=1}^{k'}\sum_{i=1}^{N}\|\xi_{u_i}^{k}\|^2+\alpha_1\exp(T)\left\|\delta t\sum_{k=1}^{k'}\xi_{q_i}^{k}\right\|^2\\&\quad+\left(C_{14}+\alpha_1\exp(T)(2+1/T)\right)\delta t\sum_{k=1}^{k'}\left\|\delta t\sum_{j=1}^{k}\xi_{q_i}^{j}\right\|^2,\end{aligned} \tag{5.65}$$

where we have also used the estimate (5.59). As in the proof of Theorem 5.1, from (5.65), we choose suitable values of α_1 and α_2 such that

$$\sum_{i=1}^{N}\left(\delta t\sum_{k=1}^{k'}\|\xi_{u_i}^k\|^2+\left\|\delta t\sum_{k=1}^{k'}\xi_{q_i}^k\right\|^2\right)\le C_{15}(\delta t)^2+C_{16}h^{2\nu}+C_{17}\delta t\sum_{k=1}^{k'}\sum_{i=1}^{N}\left\|\delta t\sum_{j=1}^{k}\xi_{q_i}^j\right\|^2. \tag{5.66}$$

Thus, it is derived by applying discrete Gronwall's lemma to (5.66) that

$$\sum_{i=1}^{N}\left(\delta t\sum_{k=1}^{k'}\|\xi_{u_i}^k\|^2+\left\|\delta t\sum_{k=1}^{k'}\xi_{q_i}^k\right\|^2\right)\le C_{18}(\delta t)^2+C_{19}h^{2\nu}. \tag{5.67}$$

Substituting (5.67) into (5.59) yields

$$\lambda_i\delta t\sum_{k=1}^{k'}\left\|\xi_{\boldsymbol{s}_i}^k\right\|^2+\left\|\delta t\sum_{k=1}^{k'}\xi_{\boldsymbol{w}_i}^k\right\|^2\le C_{20}(\delta t)^2+C_{21}h^{2\nu}. \tag{5.68}$$

Note that C_j ($18\le j\le 21$) are positive constants depending on T and the exact solutions, but they are independent of h and δt. Based on the estimates (5.67) and (5.68), we obtain the required results by the triangle rule and the linear transformation. □

6. Numerical tests

In this section, we use the proposed methods to simulate one-dimensional multi-component two-phase fluid interface problems with four type boundary conditions, and we also test a two-dimensional problem. The tested binary mixture is composed of methane (C_1) and pentane (C_5). The PR-EOS [17] is used to compute the equilibrium properties of the bulk phases, such as the densities and the chemical potentials; the detailed formulation of PR-EOS can be found in the Appendix of this paper. The binary interaction coefficients for the influence parameters are taken as $\beta_{11}=\beta_{22}=0$ and $\beta_{12}=\beta_{21}=0.5$. The mobility $\mathcal{M}$ is taken to be a constant. We define the normalized time $\widehat{t}=t\mathcal{M}$, and the simulation time period of $\widehat{t}$ is from 0 to $\widehat{t}_f$. In all tests, the temperature is kept at 260 K. Although our proposed methods are unconditionally stable and very large time step sizes are allowed to be applied in numerical simulations, we choose the suitable time step sizes in all tested examples to guarantee the accuracy instead of largest time steps. Our methods also allow us to use the adaptive time step strategy, but which will be one of our future works, so only the uniform time step approach is employed in numerical simulations of this paper. Newton's method is used as the nonlinear solver, and its stop criterion is that the total number of iterations is larger than four or the norm of relative residual errors of functions is less than 1.0e−5.

In numerical tests presented in Sections 6.1–6.4, one-dimensional domain $(0, l_x)$ is taken, where l_x is equal to 10 nm, and a uniform mesh with 100 elements is used. In one-dimensional problems, we employ the lowest order Raviart–Thomas space (RT_0), and moreover, apply the trapezoid quadrature rule for the first terms in (5.2b) and (5.2d) to decouple the system and to get explicit formula for each individual diffusive flux [41].

6.1. Neumann–Neumann problem

For the exact description of the initial–boundary condition, we denote by $\mathbf{n}^G=\left(n_1^G,\ldots,n_N^G\right)^T$ and $\mathbf{n}^L=\left(n_1^L,\ldots,n_N^L\right)^T$ the molar density of the equilibrium bulk gas and liquid phases of a mixture, respectively, under the given pressure–temperature (PT) condition at 70 bar and 260 K. The initial condition of each component is to impose the C_1 and C_5 binary mixture with the composition $0.8\mathbf{n}^L$ in the region of $(0.3l_x, 0.7l_x)$, and the rest of the domain is filled with the mixture composition $0.8\mathbf{n}^G$. In this example, we take the final simulation time $\widehat{t}_f=3\text{e}{-}17$ and the time step size is taken uniformly to be $\widehat{t}_f/10$.

Fig. 6.1 depicts the evolution of molar density of each component. It is observed that the gradient of chemical potential of each component drives diffusion of this component until the fluid system attains its equilibrium state in which chemical potential of each component equilibrates spatially. Fig. 6.2 depicts the total Helmholtz free energy varying with time steps, and the energy decay is clearly observed.

6.2. Dirichlet–Neumann problem

For the boundary conditions of molar density, we impose zero values for two components on both ends of the domain. The initial condition of each component is to impose $0.3\mathbf{n}^L$ in the entire domain, where $\mathbf{n}^L$ is the molar density of the equilibrium bulk liquid phase of the C_1 and C_5 mixture under the PT condition at 70 bar and 260 K. The final simulation time is chosen as $\widehat{t}_f=2\text{e}{-}17$, and the time step size is uniformly equal to $\widehat{t}_f/20$.

Fig. 6.3 shows the evolution profiles of molar density of each component. From these results, we observe the dynamical process that a multi-component fluid system, which is contained within a closed non-wetting medium and thus total mass

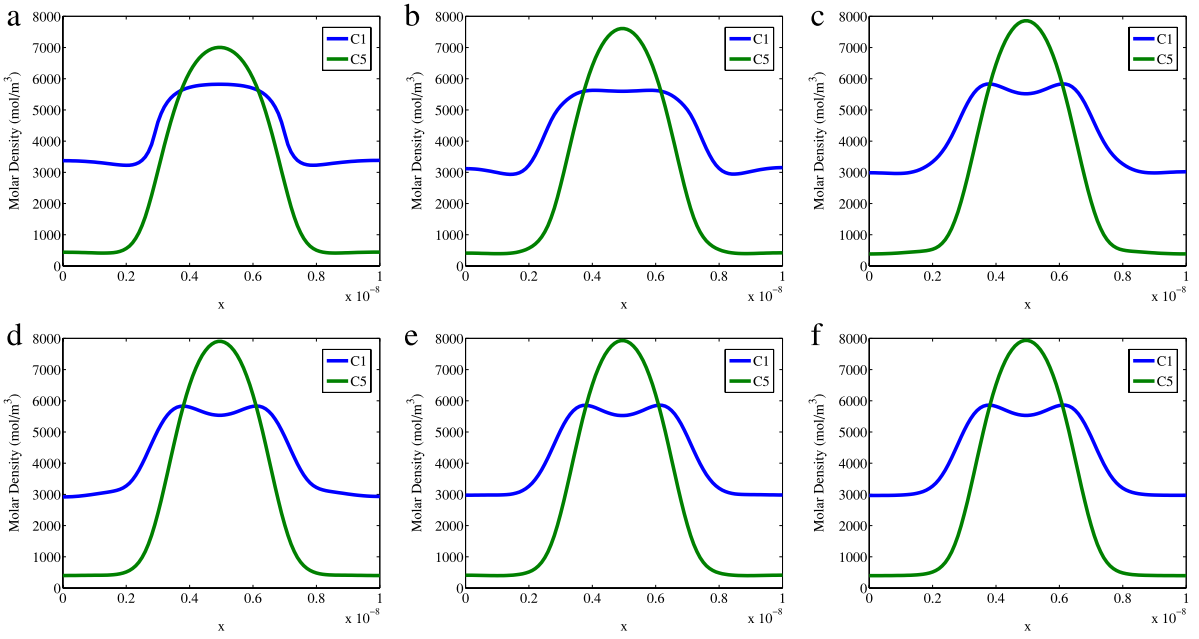

Fig. 6.1. Neumann–Neumann problem: Binary mixture molar density profiles at 260 K after 1 (a), 2 (b), 3 (c), 4 (d), 5 (e), 10 (f) time steps, respectively.

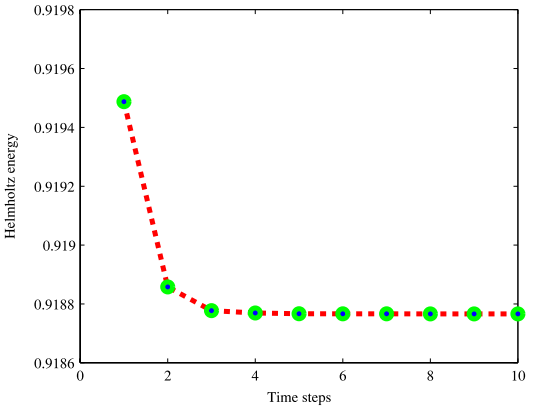

Fig. 6.2. Neumann–Neumann problem: Helmholtz free energy at 260 K.

of each component is conserved, varies from its initial state to the equilibrium. Fig. 6.4 depicts the total Helmholtz free energy, which decays with the time steps.

6.3. Dirichlet–Dirichlet problem

For the boundary conditions of molar density, we impose the left-hand-side end of the domain by $\mathbf{n}^G$ and the other end by $\mathbf{n}^L$. For the boundary conditions of chemical potential, we impose both of the ends of the domain by the chemical potential of the equilibrium bulk gas and liquid phases of a mixture under the given PT condition at 70 bar and 260 K. The initial condition of each component is to impose the binary mixture with composition $\mathbf{n}^G$ in the region of $(0, 0.5l_x)$, and the rest of the domain is filled with the mixture $\mathbf{n}^L$. In this example, the final simulation time is $\widehat{t_f} = 2\text{e}{-}16$, and the uniform time step size is equal to $\widehat{t_f}/20$.

We note that the Cahn–Hilliard system with Dirichlet–Dirichlet boundary conditions can be used as an instrument to simulate the steady diffuse interface problems and calculate the surface tension under the given equilibrium pressure and temperature; in fact, when the fluid system reaches the equilibrium, chemical potential of each component equilibrates spatially, and as a result of boundary conditions, we obtain

$$-\sum_{j=1}^{N} c_{ij}\Delta n_j + \mu_i^0(\mathbf{n}) = \mu_i^B, \quad i = 1, \ldots, N, \tag{6.1}$$

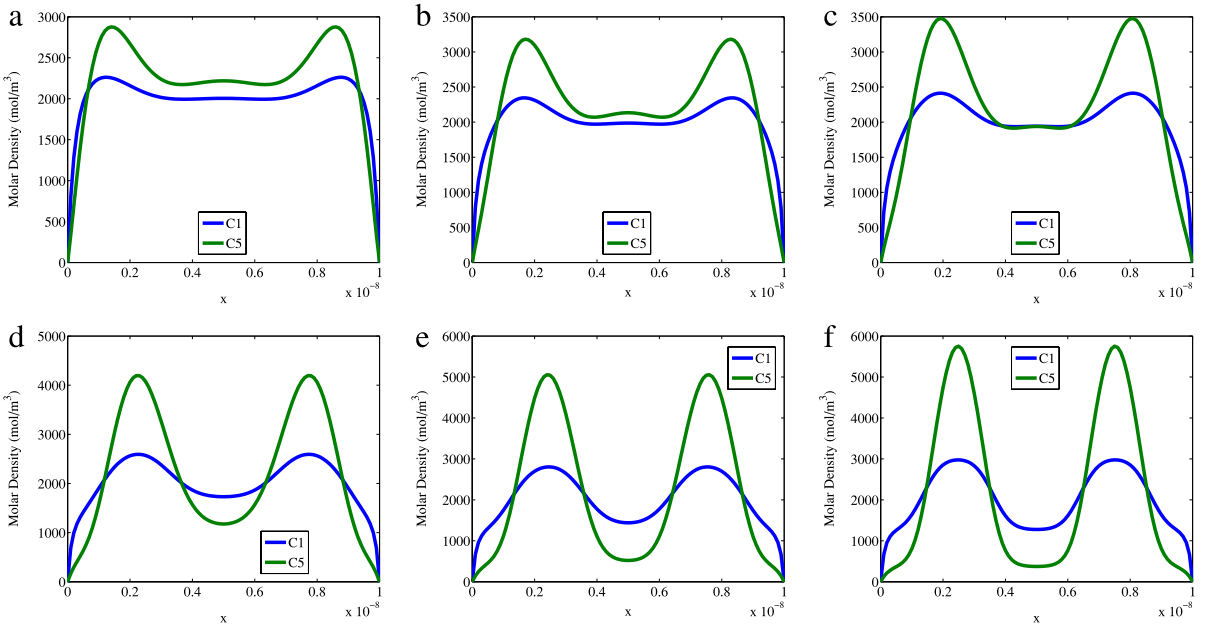

Fig. 6.3. Dirichlet–Neumann problem: Binary mixture molar density profiles at 260 K after 1 (a), 2 (b), 3 (c), 5 (d), 7 (e) and 20 (f) time steps, respectively.

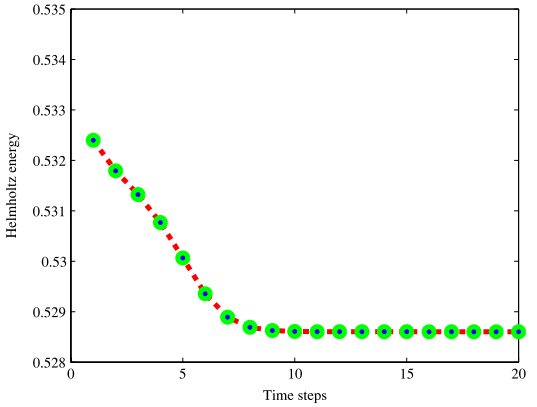

Fig. 6.4. Dirichlet–Neumann problem: Helmholtz energy at 260 K.

which are the Euler–Lagrange equations that are needed to be solved for simulating surface tension problems [18,20]. Compared to the methods of solving Euler–Lagrange equation directly, an advantage of the Cahn–Hilliard approach is that it can also provide the realistic dynamical behaviors of a fluid system varying from the initial state to the equilibrium. Fig. 6.5 illustrates the dynamical evolution of molar density of each component in the two-phase interfaces. Fig. 6.6 depicts the decay of total grand potential with time steps. These numerical results demonstrate the validity of the above theoretical analysis.

6.4. Neumann–Dirichlet problem

In this example, the initial condition of each component is to impose $0.6\mathbf{n}^L$ in the entire domain, and the boundary conditions of chemical potential is to impose both of the ends of the domain by the chemical potential of the equilibrium bulk gas and liquid phases of this binary mixture under the given PT condition at 70 bar and 260 K. The final simulation time is taken as $\widehat{t}_f = 1.5\text{e}{-16}$ and the time step size is uniformly equal to $\widehat{t}_f/20$.

Fig. 6.7 depicts the evolution of molar density of each component. These results show that the tested fluid system, which is surrounded by a fluid with constant component chemical potential, tends to equilibrium from a non-equilibrium state by component mass transfer with the external fluid. Fig. 6.8 illustrates the decay of total grand potential with time steps, which verifies the efficiency of the proposed method.

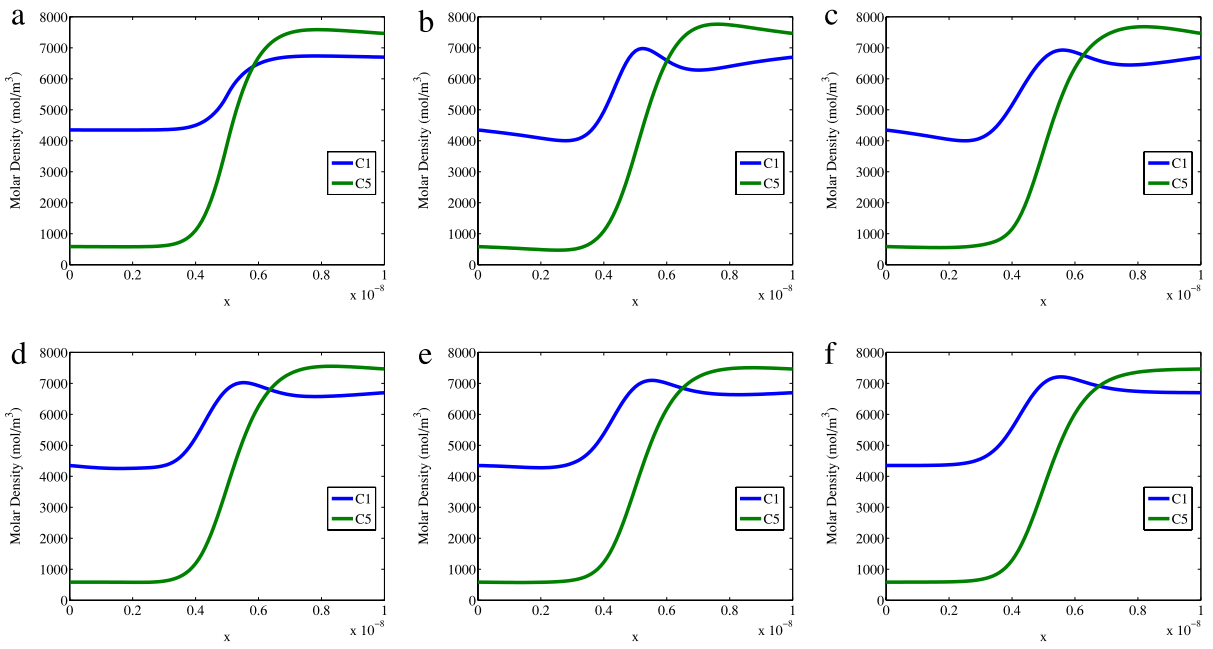

Fig. 6.5. Dirichlet–Dirichlet problem: Binary mixture molar density profiles at 260 K after 1 (a), 2 (b), 3 (c), 5 (d), 7 (e) and 20 (f) time steps, respectively.

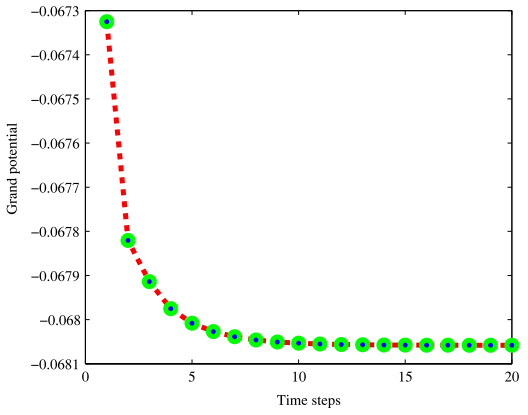

Fig. 6.6. Dirichlet–Dirichlet problem: Grand potential at 260 K.

6.5. Two-dimensional problem

We consider the problem of the binary mixture composed of methane and pentane on a two-dimensional rectangular domain $\Omega = (-l_x, l_x) \times (-l_y, l_y)$, where $l_x = l_y = 7.5$ nm. In this two-dimensional problem, we employ the lowest order Raviart–Thomas (RT_0) mixed finite element method on a triangular mesh. The initial condition is to impose the liquid density of the equilibrium bulk phase of this binary mixture under the pressure 70 bar and temperature 260 K in the region of $[-0.25l_x, 0.25l_x] \times [-0.25l_y, 0.25l_y]$, and the rest of the domain is filled with the gas of this binary mixture under the same pressure and temperature conditions. In Fig. 6.9, we depict the initial molar density distribution of methane and pentane on the used triangular mesh. The Neumann–Neumann boundary condition is chosen on the entire boundary of the domain. In this example, the final simulation time is taken as $\widehat{t_f} = 1.5\text{e}{-17}$ and the time step size is uniformly equal to $\widehat{t_f}/5$. Fig. 6.10 shows the molar density distribution of methane and pentane at different time steps.

7. Conclusions

We have studied two-phase dynamic interface models for multi-component fluids, which are formulated by the Cahn–Hilliard system with Peng–Robinson equation of state and various boundary conditions. The corresponding minimum problems of Helmholtz free energy and grand potential are also derived for the realistic thermodynamic systems. The mixed weak forms of the resulted Cahn–Hilliard systems with various boundary conditions are formulated such that we can

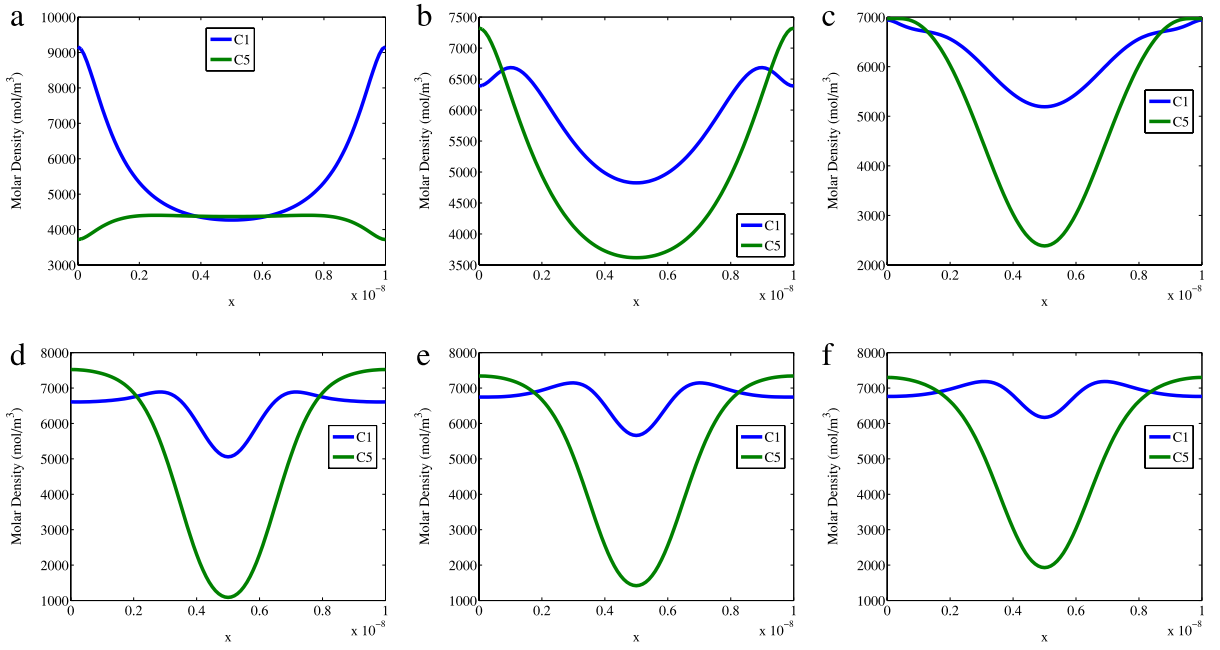

Fig. 6.7. Neumann–Dirichlet problem: Binary mixture molar density profiles at 260 K after 1 (a), 2 (b), 3 (c), 5 (d), 13 (e) and 20 (f) time steps, respectively.

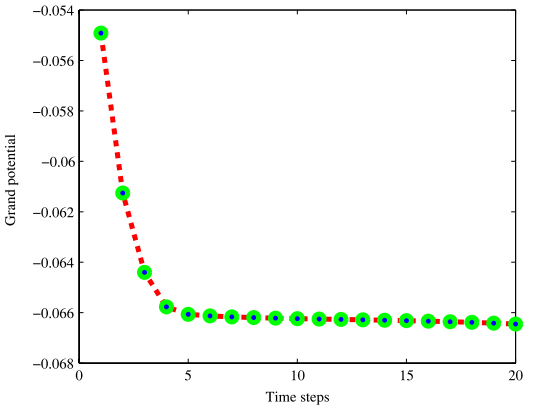

Fig. 6.8. Neumann–Dirichlet problem: Grand potential at 260 K.

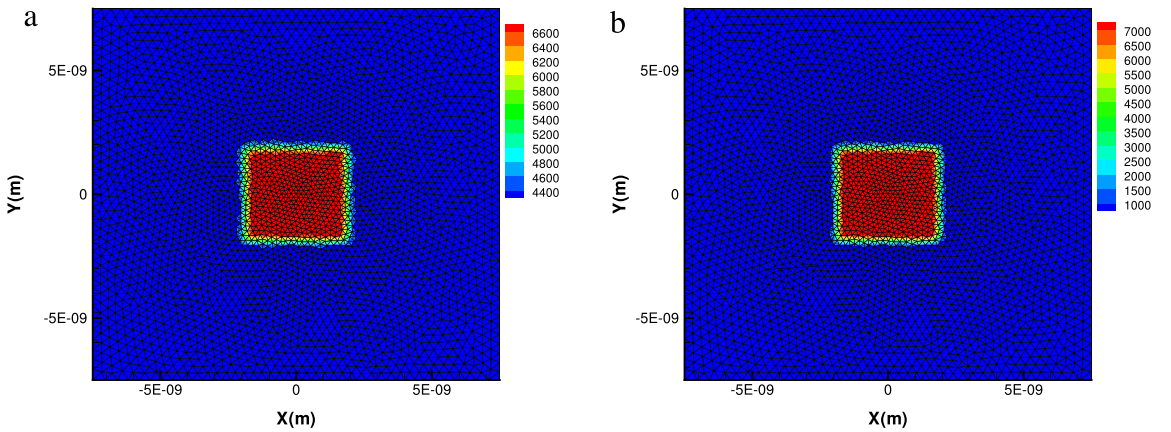

Fig. 6.9. Initial molar density distribution of methane and pentane on 2D triangular mesh: (a) methane molar density (in mol/m^3); (b) pentane molar density (in mol/m^3).

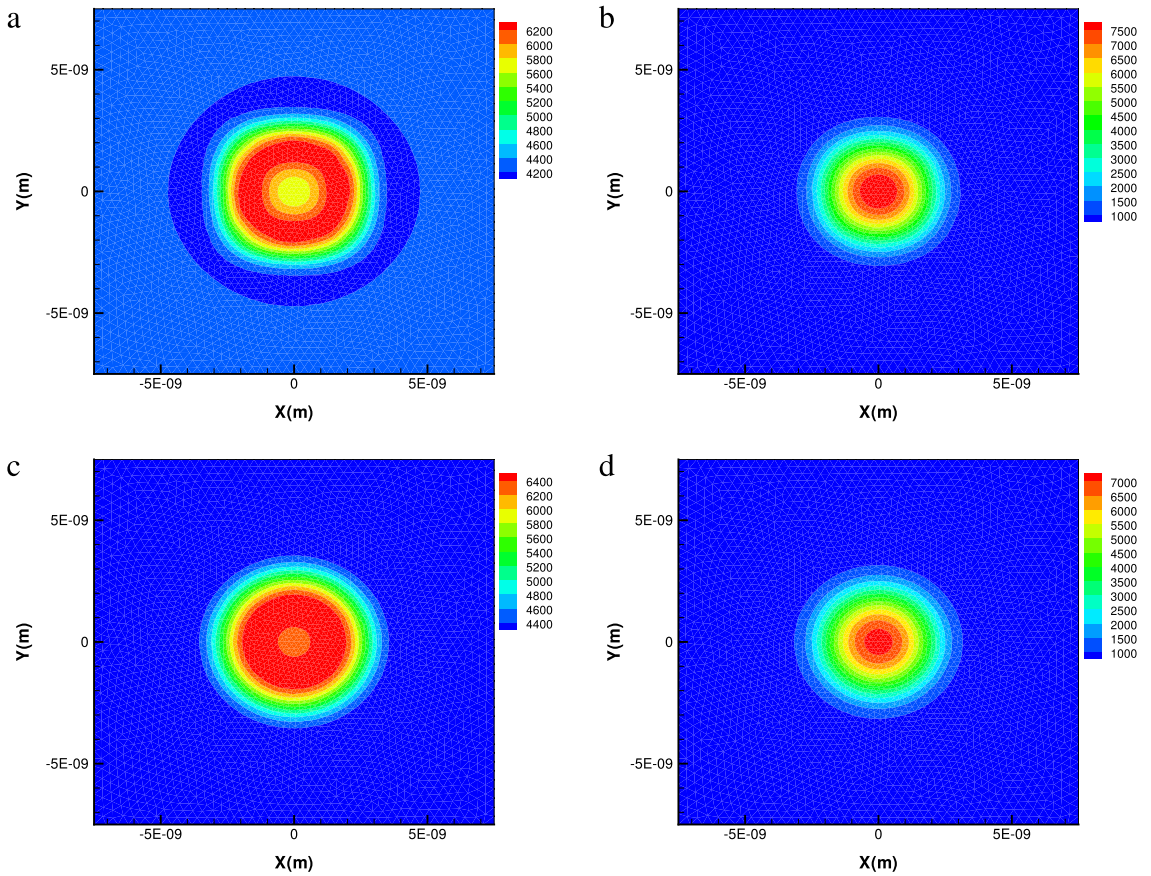

Fig. 6.10. Molar density distribution of methane and pentane: (a) methane molar density (in mol/m^3) after 2 time steps; (b) pentane molar density (in mol/m^3) after 2 time steps; (c) methane molar density (in mol/m^3) after 5 time steps; (d) pentane molar density (in mol/m^3) after 5 time steps.

conveniently use the mixed finite element methods since these methods are capable of achieving very accurate and stable approximations of both the primary unknown and its flux across grid-cell. For sake of reducing the full coupling property of our models, we use a linear transformation to decouple the relations between component densities, and furthermore, we propose a semi-implicit unconditionally stable time schemes. The proposed methods simplify the models and weaken strong nonlinearity, so we can solve the Cahn–Hilliard system by a decoupled way. As a result, the proposed methods can significantly reduce the computational cost and memory requirements in numerical simulations. We have also estimated the discrete errors of mixed finite element approximations. Numerical results verify the theoretical results and the efficiency of the proposed methods.

Appendix

In this appendix, we will describe the computations of Helmholtz free energy density $f_0(\mathbf{n})$ of a homogeneous fluid and the parameters used in Peng–Robinson equation of state.

The Helmholtz free energy density $f_0(\mathbf{n})$ of a homogeneous fluid is formulated by a thermodynamic model as

$$f_0(\mathbf{n}) = f_0^{ideal}(\mathbf{n}) + f_0^{excess}(\mathbf{n}),$$

$$f_0^{ideal}(\mathbf{n}) = RT \sum_{i=1}^{N} n_i \left(\ln n_i - 1\right),$$

$$f_0^{excess}(\mathbf{n}) = -nRT \ln\left(1 - bn\right) + \frac{a(T)n}{2\sqrt{2}b} \ln\left(\frac{1 + (1 - \sqrt{2})bn}{1 + (1 + \sqrt{2})bn}\right),$$

where $n = \sum_{i=1}^{N} n_i$, T is the temperature of the mixture and R is the universal gas constant. Here, $a(T)$ and b are the energy parameter and the covolume, respectively, and these parameters can be calculated with the mixture composition and temperature. Denote by P the pressure of the mixture and denote by T_{c_i} and P_{c_i} the critical temperature and pressure,

respectively, of component i. For the ith component, let the reduced temperature be $T_{r_i} = T/T_{c_i}$. Define the mole fraction $z_i = n_i/n$. The parameters a_i and b_i are calculated as

$$a_i = 0.45724\frac{R^2T_{c_i}^2}{P_{c_i}}\left[1 + m_i(1 - \sqrt{T_{r_i}})\right]^2, \qquad b_i = 0.07780\frac{RT_{c_i}}{P_{c_i}}.$$

The coefficients m_i are calculated by the following formulations

$$m_i = 0.37464 + 1.54226\omega_i - 0.26992\omega_i^2, \quad \omega_i \le 0.49,$$
$$m_i = 0.379642 + 1.485030\omega_i - 0.164423\omega_i^2 + 0.016666\omega_i^3, \quad \omega_i > 0.49,$$

where ω_i is the acentric factor. Finally, $a(T)$ and b are calculated by

$$a(T) = \sum_{i=1}^{N}\sum_{j=1}^{N} z_iz_j\left(a_ia_j\right)^{1/2}(1 - k_{ij}), \qquad b = \sum_{i=1}^{N} z_ib_i,$$

where k_{ij} the given binary interaction coefficients for the energy parameters.

The pure component influence parameters c_i are given by

$$c_i = a_ib_i^{2/3}\left[\alpha_i(1 - T_{r_i}) + \gamma_i\right],$$

where α_i and γ_i are the coefficients correlated merely with the acentric factor ω_i of the component i by the following relations

$$\alpha_i = -\frac{10^{-16}}{1.2326 + 1.3757\omega_i}, \qquad \gamma_i = \frac{10^{-16}}{0.9051 + 1.5410\omega_i}.$$

The Peng–Robinson equation of state (PR-EOS) [17] is given as the following form:

$$P = \frac{RT}{v - b} - \frac{a(T)}{v(v + b) + b(v - b)},$$

where v is the molar volume of a mixture.

References

[1] A. Firoozabadi, Thermodynamics of Hydrocarbon Reservoirs, McGraw-Hill, New York, 1999.
[2] L.W. Lake, Fundamentals of Enhanced Oil Recovery, Society of Petroleum Engineers, 1986.
[3] C. Dawson, S. Sun, M.F. Wheeler, Compatible algorithms for coupled flow and transport, Comput. Methods Appl. Mech. Engrg. 193 (2004) 2565–2580.
[4] S. Sun, M.F. Wheeler, Symmetric and nonsymmetric discontinuous Galerkin methods for reactive transport in porous media, SIAM J. Numer. Anal. 43 (1) (2005) 195–219.
[5] V. Girault, S. Sun, M.F. Wheeler, I. Yotov, Coupling discontinuous Galerkin and mixed finite element discretizations using mortar finite elements, SIAM J. Numer. Anal. 46 (2) (2008) 949–979.
[6] S. Sun, J. Liu, A locally conservative finite element method based on enrichment of the continuous Galerkin method, SIAM J. Sci. Comput. 31 (4) (2009) 2528–2548.
[7] M.F. Wheeler, T. Wick, W. Wollner, An augmented-lagrangian method for the phase-field approach for pressurized fractures, Comput. Methods Appl. Mech. Engrg. 271 (2014) 69–85.
[8] J. Shen, C. Wang, X. Wang, S.M. Wise, Second-order convex splitting schemes for gradient flows with Ehrlich–Schwoebel type energy: application to thin film epitaxy, SIAM J. Numer. Anal. 50 (1) (2012) 105–125.
[9] J. Shen, X. Yang, Decoupled energy stable schemes for phase-field models of two-phase complex fluids, SIAM J. Sci. Comput. 36 (1) (2014) B122–B145.
[10] J. Kim, Phase-field models for multi-component fluid flows, Commun. Comput. Phys. 12 (3) (2012) 613–661.
[11] D.M. Anderson, G.B. McFadden, A.A. Wheeler, Diffuse-interface methods in fluid mechanics, Annu. Rev. Fluid Mech. 30 (1) (1998) 139–165.
[12] J. Kim, A generalized continuous surface tension force formulation for phase-field models for multi-component immiscible fluid flows, Comput. Methods Appl. Mech. Engrg. 198 (37) (2009) 3105–3112.
[13] K.E. Teigen, P. Song, J. Lowengrub, A. Voigt, A diffuse-interface method for two-phase flows with soluble surfactants, J. Comput. Phys. 230 (2) (2011) 375–393.
[14] P. Boyanovaa, M. Neytcheva, Efficient numerical solution of discrete multi-component Cahn–Hilliard systems, Comput. Math. Appl. 67 (2014) 106–121.
[15] B. Nestler, A. Choudhury, Phase-field modeling of multi-component systems, Curr. Opin. Solid State Mater. Sci. 15 (3) (2011) 93–105.
[16] F. Chen, J. Shen, Efficient energy stable schemes with spectral discretization in space for anisotropic Cahn–Hilliard systems, Commun. Comput. Phys. 13 (2013) 1189–1208.
[17] D. Peng, D.B. Robinson, A new two-constant equation of state, Ind. Eng. Chem. Fundam. 15 (1) (1976) 59–64.
[18] J. Kou, S. Sun, An adaptive finite element method for simulating surface tension with the gradient theory of fluid interfaces, J. Comput. Appl. Math. 255 (2014) 593–604.
[19] Z. Qiao, S. Sun, Two-phase fluid simulation using a diffuse interface model with Peng–Robinson equation of state, SIAM J. Sci. Comput. 36 (4) (2014) B708–B728.
[20] J. Kou, S. Sun, X. Wang, Efficient numerical methods for simulating surface tension of multi-component mixtures with the gradient theory of fluid interfaces, Comput. Methods Appl. Mech. Engrg. (2014) http://dx.doi.org/10.1016/j.cma.2014.10.023.
[21] J.W. Cahn, J.E. Hilliard, Free energy of a nonuniform system: I. Interfacial free energy, J. Chem. Phys. 28 (1958) 258–267.
[22] C.M. Elliott, H. Garcke, Diffusional phase transitions in multicomponent systems with a concentration dependent mobility matrix, Physica D 109 (1997) 242–256.
[23] P.M.W. Cornelisse, The square gradient theory applied-simultaneous modelling of interfacial tension and phase behaviour (Ph.D. thesis), TU Delft, The Netherlands, 1997.
[24] D.A. Cogswell, A phase-field study of ternary multiphase microstructures (Ph.D. thesis), MIT, USA, 2010.
[25] L. de Sobrino, J. Peternelj, On capillary waves in the gradient theory of interfaces, Can. J. Phys. 63 (1985) 131–134.
[26] H.G. Lee, J.-W. Choi, J. Kim, A practically unconditionally gradient stable scheme for the N-component Cahn–Hilliard system, Physica A 391 (2012) 1009–1019.

[27] C. Miqueu, B. Mendiboure, A. Graciaa, J. Lachaise, Modeling of the surface tension of multicomponent mixtures with the gradient theory of fluid interfaces, Ind. Eng. Chem. Res. 44 (9) (2005) 3321–3329.
[28] A.I. Rusanov, A.K. Shchekin, D.V. Tatyanenko, Grand potential in thermodynamics of solid bodies and surfaces, J. Chem. Phys. 131 (2009) 161104.
[29] K. Bao, Y. Shi, S. Sun, X.-P. Wang, A finite element method for the numerical solution of the coupled Cahn–Hilliard and Navier–Stokes system for moving contact line problems, J. Comput. Phys. 231 (24) (2012) 8083–8099.
[30] S. Vedantam, B.S.V. Patnaik, Efficient numerical algorithm for multiphase field simulations, Phys. Rev. E 73 (2006) 016703. 1-8.
[31] C.E. Krill III, L.-Q. Chen, Computer simulation of 3-D grain growth using a phase-field model, Acta Mater. 50 (2002) 3057–3073.
[32] H. Gomez, X. Nogueira, An unconditionally energy-stable method for the phase field crystal equation, Comput. Methods Appl. Mech. Engrg. 249 (2012) 52–61.
[33] L. Cueto-Felgueroso, J. Peraire, A time-adaptive finite volume method for the Cahn–Hilliard and Kuramoto–Sivashinsky equations, J. Comput. Phys. 227 (2008) 9985–10017.
[34] R. Guo, Y. Xia, Y. Xu, An efficient fully-discrete local discontinuous Galerkin method for the Cahn–Hilliard–Hele–Shaw system, J. Comput. Phys. 264 (2014) 23–40.
[35] Yinhua Xia, Yan Xu, Chi-Wang Shu, Local discontinuous Galerkin methods for the Cahn–Hilliard type equations, J. Comput. Phys. 227 (2007) 472–491.
[36] X. Feng, A. Prohl, Analysis of a fully discrete finite element method for the phase field model and approximation of its sharp interface limits, Math. Comp. 73 (246) (2003) 541–567.
[37] H. Gomez, A. Reali, G. Sangalli, Accurate, efficient, and (iso)geometrically flexible collocation methods for phase-field models, J. Comput. Phys. 262 (2014) 153–171.
[38] G.N. Wells, E. Kuhl, K. Garikipati, A discontinuous Galerkin method for the Cahn–Hilliard equation, J. Comput. Phys. 218 (2006) 860–877.
[39] S. Sun, B. Riviere, M.F. Wheeler, A combined mixed finite element and discontinuous Galerkin method for miscible displacement problem in porous media, in: Recent Progress in Computational and Applied PDEs, Conference Proceedings for the International Conference held in Zhangjiajie in, 2001, pp. 321–348.
[40] F. Brezzi, M. Fortin, Mixed and Hybrid Finite Element Methods, Springer Verlag, 1991.
[41] T. Arbogast, M.F. Wheeler, I. Yotov, Mixed finite elements for elliptic problems with tensor coefficients as cell-centered finite differences, SIAM J. Numer. Anal. (1997) 828–852.
[42] R.A. Raviart, J.M. Thomas, A mixed finite element method for 2nd order elliptic problems, in: Mathematical Aspects of the Finite Element Method, in: Lecture Notes in Mathematics, vol. 606, 1977, pp. 292–315.
[43] R.A. Raviart, J.M. Thomas, Primal hybrid finite element methods for 2nd order elliptic equations, Math. Comp. 31 (1977) 391–413.
[44] F.A. Radu, I.S. Pop, P. Knabner, Error estimates for a mixed finite element discretization of some degenerate parabolic equations, Numer. Math. 109 (2008) 285–311.